

GATING MECHANISMS IN HYPERPOLARIZATION-
ACTIVATED CYCLIC NUCLEOTIDE-GATED ION
CHANNELS

By
Sriharsha Vemana

A DISSERTATION

Presented to the Neuroscience Graduate Program

And the Oregon Health and Science University

School of Medicine

In partial fulfillment of

The requirements for the degree of

Doctor of Philosophy

July 2007


School of Medicine
Oregon Health & Science University

CERTIFICATE OF APPROVAL


This is to certify that the Ph.D. dissertation of
SRIHARSHA VEMANA
has been approved




Advisor, (Hans Peter Larsson PhD)




Member, (Ronald Lane Brown PhD)



Member, (James Maylie PhD)



Member, (John Adelman PhD)



Member, (Show-Ling Shyng PhD)

Table of Contents

I. CHAPTER 1	1
<i>Introduction</i>	<i>1</i>
A. OVERVIEW	1
B. PHYSIOLOGY AND FUNCTION OF HCN CHANNELS	2
<i>a. The 'Funny' current</i>	2
<i>b. Cloning of HCN channels</i>	4
<i>c. Biophysical properties among HCN channels</i>	5
i. Mammalian HCN channels	6
ii. Non-mammalian HCN channels	7
iii. cAMP modulation.....	7
<i>d. HCN channel expression in the body</i>	8
i. Subunit assembly	9
<i>e. Physiological role</i>	10
i. Effects of HCN knock-out.	11
C. STRUCTURAL BASES FOR THE FUNCTIONAL PROPERTIES OF HCN CHANNELS	11
<i>a. The pore domain of HCN channels</i>	11
i. Permeation and Blocking properties	11
ii. Structure of the HCN pore	13
iii. HCN channels have an intracellular gate	14
<i>b. The CNBD domain in HCN channels</i>	15
i. CNBD and HCN channel opening	15
ii. Answers from the HCN2 CNBD domain crystal structure	17
<i>c. Voltage-dependent gating of HCN channels</i>	17
i. Hodgkin and Huxley	18
ii. Gating particles and gating current	21
iii. S4 is the voltage sensor in Kv channels	23
<i>d. Models for HCN channel gating</i>	25
i. Kir model for HCN gating	25
ii. HERG model for HCN gating: recovery from an inactivated state.....	26
iii. KAT1 model for HCN gating: activation from a closed state.....	27
iv. Early structure/function studies of HCN S4.....	28
v. Coupling between S4 and the channel gate	30
vi. Crystal Structures.....	30
vii. Future Directions for HCN study.....	32
II. CHAPTER 2	34
<i>S4 movement in a mammalian HCN channel</i>	34
A. ABSTRACT	35
B. INTRODUCTION	37
C. METHODS.....	40
<i>a. molecular biology</i>	40
<i>b. Electrophysiology</i>	41
<i>c. Two-electrode voltage-clamp technique</i>	41
<i>d. Patch voltage-clamp technique</i>	42

<i>e. Cysteine Labeling and Accessibility Studies</i>	42
<i>f. MTS Reagent Stability</i>	45
D. RESULTS	49
<i>a. S4 is the voltage sensor for HCN1</i>	49
<i>b. The range of movement for S4</i>	57
<i>c. The COOH terminus and gating differences between HCN1 and spHCN</i>	61
E. DISCUSSION	65
III. CHAPTER 3	77
<i>Intracellular Mg²⁺ is a voltage dependent pore blocker of HCN channels</i>	77
A. ABSTRACT	79
B. INTRODUCTION	80
C. METHODS	83
<i>a. Molecular Biology</i>	83
<i>b. Electrophysiology</i>	83
D. RESULTS	85
<i>a. Instantaneous rectification is not due to an intrinsic voltage-dependent process</i>	85
<i>b. Intracellular Mg²⁺ blocks HCN currents at physiological concentrations</i>	91
<i>c. Mg²⁺ blocks HCN currents in a voltage dependent manner</i>	94
<i>d. The effect of a pore mutation suggests that Mg²⁺ binds to the selectivity filter</i>	99
<i>e. Magnesium causes inward rectification in a permanently-open HCN channel</i>	102
E. DISCUSSION	105
IV. DISCUSSION	112
A. S4 IS THE VOLTAGE SENSOR	112
<i>a. S4 movement in HCN1 and Shaker</i>	113
<i>b. Models for S4 conformational changes</i>	115
<i>c. Crystal Structures</i>	117
<i>d. Future Experiments</i>	120
B. Mg²⁺ ACTS AS AN 'EXTRINSIC' RECTIFIER IN HCN CHANNELS	120
<i>a. Mg²⁺ inside the cell</i>	121
<i>b. Mg²⁺ block of ion channels</i>	121
<i>c. Mechanism of HCN block by Mg²⁺</i>	122
<i>d. Mg²⁺ and HCN, the physiological significance</i>	123
<i>e. Future Experiments</i>	124
V. SUMMARY AND CONCLUSIONS	125
VI. REFERENCES	127

LIST OF FIGURES

- Figure 1.** Stability of MTSET at room temperature and on ice
- Figure 2.** Membrane topology and sequence alignment of HCN1 channels
- Figure 3.** State-dependent accessibility of S253C
- Figure 4.** State-dependent accessibility of L254C
- Figure 5.** State-dependent accessibility of three S4 residues
- Figure 6.** The C-terminus is necessary for inactivation in spHCN channels
- Figure 7.** A model of the voltage-dependent movements of S4 in the HCN1 channel and the spHCN channel
- Figure 8.** Larger state-dependent modification of T249C at more hyperpolarized potentials
- Figure 9.** HCN channels show rectification in cell-attached patches
- Figure 10.** HCN1 and HCN2 tail currents increase in amplitude after excision
- Figure 11.** Patch cramming reduces the amplitude of the outward currents back to cell attached levels
- Figure 12.** Physiological concentrations of intracellular magnesium block HCN outward current more than spermine or spermadine
- Figure 13.** Mg^{2+} blocks HCN outward currents at physiological concentrations
- Figure 14.** Voltage dependence of Mg^{2+} block
- Figure 15.** The mutant C347S altered the magnesium affinity in HCN1 channels
- Figure 16.** Magnesium causes inward rectification in a permanently-open HCN channel
- Figure 17.** Putative location of the Mg^{2+} binding site in the pore
- Figure 18.** Mg^{2+} blocks a voltage-independent component of the current at positive voltages

LIST OF TABLES

Table 1. Modification rate constants for mutants R247C, T249C, I251C, S253C, and L254C.

LIST OF ABBREVIATIONS

- Adenosine triphosphate (ATP)
- Arabidopsis Thaliana Potassium channel (KAT1)
- Barium (Ba^{2+})
- Chloride (Cl^-)
- Cyclic adenosine-mono-phosphate (cAMP)
- Cyclic guanosine mono-phosphate (cGMP)
- Cyclic nucleotide-binding domain (CNBD)
- Cyclic nucleotide-gated channels (CNG)
- Fourth transmembrane domain (S4)
- Human Ether-a-go-go Related Gene (HERG)
- Hyperpolarization-activated cyclicnucleotide-gated channels (HCN)
- Hyperpolarization-activated cyclicnucleotid-gated channel cloned from sea urchin sperm (spHCN)
- Inwardly-rectifying Potassium channel (Kir)
- K_v channel from archeabacterium *Aeropyrum Pernix* (*KvAP*)
- Magnesium (Mg^{2+})
- Potassium (K^+)
- Potassium Channel From Streptomyces Lividans (Kcsa)
- Renal Outer Medullary Potassium channel (ROMK1)
- Sino-atrial node (SA)
- Shaker Potassium channel 1.2 ($K_v1.2$)
- Sodium (Na^+)
- Substituted Cysteine Accessibility Method (SCAM)
- Trimethylammonioethylmethane thiosulphonate (MTSET)
- Voltage-dependent K^+ channel (K_v)

ACKNOWLEDGEMENTS

I was lucky in having Peter as an advisor. He is, without a doubt, the best student advisor a graduate student could possibly have. I do hope that we keep a friendship as I move on. Peter is the second most patient person I have met, the first being my father. In fact, I may be the only person in the entire world to have pushed both of them past their limit on several occasions...

I would also like to thank my family for unconditional support. I do wish they were closer to Portland, but I appreciate the time spent with them.

My brothers, who are both medical doctors, have been invaluable in keeping things in perspective with their constant questions to the clinical relevance to "whatever it is that I do"

Of course, my fellow lab members, all friends for life. Even if experiments were not going well, it was always fun to spend time with them

Also, all the friends I made in Portland, and the old ones who moved here, who always made me feel like I was 17

And finally, I would like to thank Portland Oregon. I don't think I would have survived without the forests, mountains, lakes, rivers, and beaches that surround the city.

peace

Abstract

Hyperpolarization-activated cyclic nucleotide-gated ion channels (HCN) are gated by voltage, that is, they are able to detect changes in voltage and convert that into work for opening and closing (gating) the channel gate. The focus of this thesis was to investigate the gating mechanisms in HCN channels. Results from these experiments revealed that HCN channels have a voltage sensor (S4) similar to Kv channels but have reversed gating. This makes up the first half of the thesis. In addition, the outward currents through HCN channels are susceptible to a voltage-dependent block by intracellular Mg^{2+} . The experiments relating to the Mg^{2+} block make up the second half of the thesis.

HCN channels mediate an inward cation current that contributes to spontaneous rhythmic firing activity in the heart and brain. These channels share homology with depolarization-activated Kv channels, including six transmembrane domains (S1-S6) and a positively charged S4 segment. The S4 domain has been shown to function as the voltage sensor and undergo a voltage-dependent movement in the Shaker K^+ channel. Experiments making up the first half of the thesis, incorporated the substituted cysteine accessibility method in conjunction with two-electrode voltage clamp to test for state dependent movement in the S4 domain of HCN1. Six cysteine mutations (R247C, T249C, I251C, S253C, L254C, and S261C) were used to assess S4 movement of the heterologously expressed HCN1 channel in *Xenopus* oocytes. State-dependent accessibility was found for four residues, T249C and S253C from the extracellular solution and

L254C and S261C from the intracellular solution. These results suggest that the role of S4 as the voltage sensor in HCN channels is conserved.

HCN channels are also gated by cyclic nucleotides, specifically cAMP, which binds to a cyclic nucleotide binding domain (CNBD) located in the HCN C-terminus. The binding of cAMP relieves a tonic inhibition of channel opening caused by the CNBD. All HCN channels have a CNBD, but different HCN isoforms exhibit varying levels of sensitivity to cAMP modulation. In an attempt to find the structural basis for this difference in sensitivity, the C-terminus was deleted from HCN1 and a nonmammalian HCN channel, spHCN, whose currents inactivate during low intracellular levels of cAMP. HCN1 channels do not inactivate are relatively insensitive to changes in cAMP concentrations. The C-terminus deleted spHCN channel appeared similar to the C-terminus-deleted HCN1 channel, suggesting that differences in gating between spHCN and HCN1 are due to differences in the C-terminus or interactions between the C-terminus and the rest of the channel.

The second half of the thesis builds upon the fact that HCN channels are activated by membrane hyperpolarization mediating time-dependent, inward-rectifying currents, gated by the movement of the voltage sensor, S4. However, inward rectification of the HCN currents is not only observed in the time-dependent HCN currents, but also in the instantaneous HCN tail currents. Experiments, included in the second half of the thesis, show that intracellular

Mg²⁺ functions as a voltage-dependent blocker of HCN channels, acting to reduce the instantaneous outward currents. The affinity of HCN channels for Mg²⁺ is in the physiological range, with Mg²⁺ binding with an IC₅₀ of 0.53 mM at +50 mV in HCN2 channels and an IC₅₀ of 0.82 mM at +50 mV for HCN1 channels. Mg²⁺ block was also found to be voltage dependent with an effective electrical distance for the Mg²⁺ binding site of 0.19. Removing a cysteine in the selectivity filter reduced the affinity for Mg²⁺ suggesting that this residue forms part of the binding site deep within the pore. Mg²⁺ is also able to block both the time-dependent and time-independent outward currents in HCN channels. Mg²⁺ is proposed to act as an 'extrinsic' gating mechanism which complements the primary S4 mediated voltage-dependent gating of an HCN channel

I. Chapter 1

Introduction

A. Overview

Our everyday actions, from the way we perceive the world around us to the actions we choose to interact with the world around us, have their basis in the conduction of electrical signals within our physical bodies. The foundation for these electrical signals are ion channels, whose passage of ions into and out of cells, mediate the signals and responses of our nervous system. Essentially protein pores embedded in the cellular membrane, ion channels possess the ability to transduce a specific stimulus into the conduction of select ions through its pore. This stimulus may be in the form of mechanical force, chemicals, or voltage, all of which are coupled to the opening or closing of a channel gate (a process called gating), which acts to help control the movement of ions through the channel pore. In the case of voltage-gated ion channels, work by Hodgkin and Huxley as well as Cole and Curtis, performed a little over a half a century ago, set the stage for much of the present research into voltage-gated ion channels[1, 2]. Hodgkin and Huxley proposed the existence of charged gating particles (i.e. voltage sensors) that move through the membrane in response to voltage [1], converting this work into the opening and closing of a channel gate. Subsequent research validated this claim, by showing the existence of a positively charged domain (the putative voltage sensor) within voltage-gated ion channels that does in fact move through the membrane in response to voltage. It

is known that in most voltage-gated ion channels, positive voltage inside the cell is the stimulus that opens the channel gate. Thus, these channels are depolarization activated ion channels. The question remains, however, as to how this movement is linked (i.e. coupled) to the opening and closing of the channel gate. This question became even more intriguing with the discovery of a class of ion channels that open their gate in response to negative voltage inside the cells: hyperpolarization-activated ion channels. In addition to voltage, these hyperpolarization-activated ion channels are also modified by the binding of intracellular molecules such as cAMP. These channels were thus named hyperpolarization-activated cyclic-nucleotide gated (HCN) ion channels. Subsequent study on HCN channels focused on questions such as the identification of the voltage sensor in HCN channels and the gating mechanism in HCN channels. These questions were the primary focus of work contained in this thesis, culminating in the publication of the two manuscripts found in the chapters following the introduction. Though a definitive resolution to the coupling question remains to be found for both hyperpolarization-activated channels and depolarization-activated channels, the following thesis dissertation offers some insight into the mechanism of gating in HCN channels.

B. Physiology and Function of HCN channels

a. The 'Funny' current

Hyperpolarization-activated cyclic nucleotide gated ion channels (HCN) were first identified due to their unusual physiological properties. Recordings from

two electrode voltage-clamped sino-atrial preparations [3, 4] found a slowly rising depolarizing current that activated at hyperpolarized potentials and seemed to mediate the control of cardiac action potential frequency by autonomic neurotransmitters. Sympathetic stimulation seemed to increase the rate of rise for this depolarizing current in the heart (also referred to as diastolic (or pacemaker) depolarization), while parasympathetic stimulation decreased the rate of rise [5]. This current was labeled I_f , for 'funny' current, due to its anomalous behavior when compared to conventional depolarization activated K^+ channels. The homologous current found in neurons was labeled I_h . Initial attempts to characterize the I_f current focused on distinguishing between a time- and voltage-dependent change in membrane conductance versus a shift in the driving force caused by ion accumulation or depletion [6]. Two studies showed increases in the membrane conductance supporting the view of a separate I_h conductance [7, 8]. Further support for the membrane conductance basis of the current came from single-channel recordings, which identified very small single channel events (1pS), that underlie I_f in rabbit sino-atrial node cells [9], strongly supporting the concept of a voltage-gated membrane conductance. Further analysis of I_f current revealed that it was a nonspecific cation current carried by both K^+ and Na^+ and thus had a reversal potential around -30mV [7, 10-12]. In addition, I_f slowly activated upon hyperpolarization to voltages ranging from -35mV to -60mV. Subsequent studies identified I_f in several different cardiac and neuronal cell types [13, 14], however, the molecular basis for this current

was not studied in detail until the cloning of the HCN channel family, which occurred almost two decades later.

b. Cloning of HCN channels

The study of the molecular basis for the ‘funny’ current began in earnest following the cloning from the mouse brain [15] of the first isoform of the HCN channel family, mHCN1. Other isoforms of the HCN channels were subsequently cloned, including HCN2, HCN3 and HCN4 [16, 17]. These channels have been cloned from a variety of mammalian species (mouse, human, rat, and rabbit). Non-mammalian HCN channels have also been cloned, including spHCN1[18] and more recently, spHCN2[19]. Both of these channels were cloned from sea urchin sperm. HCN channels exhibit several shared motifs with members of the super-family of voltage-gated K^+ ion channels, including a four subunit tetrameric superstructure, with each subunit made up of six transmembrane domains (S1-S6), a positively-charged S4 domain, and a similar pore domain (S5-S6) that includes the GYG signature motif that is a hallmark for K^+ selectivity. Despite the similarities to voltage-gated K^+ channels, such as Shaker, HCN channels show some divergence from these channels, for example, the presence of a cyclic-nucleotide binding domain (CNBD) at the cytoplasmic side of HCN channels towards the C-terminus, similar to that of CNG channels (cyclic-nucleotide gated channels, which have no voltage dependence of activation or K^+ selectivity).

The homology for the protein sequence between the four mammalian HCN channels is high: 56-60% for the whole protein and up to 80-90% for the core region, including S1 through the CNBD. There is a 52-54% sequence similarity between mammalian HCN channels and spHCN1 for the core region of the protein. When compared to other types of channels, HCN channels have the most homology to ion channels in the superfamily of voltage-gated ion channels that have a cyclic-nucleotide binding domain, including EAG-related channels, CNG channels, and the plant inward rectifiers, such as KAT1.

c. Biophysical properties among HCN channels

Under whole-cell voltage clamp of HCN channels in HEK293 cells, steps to hyperpolarized potentials cause a slow inward current, whose rate of activation and amplitude increase as the level of hyperpolarization increases [16]. This inward current is carried by both Na^+ and K^+ , a fact reflected in the -30 mV reversal potential for HCN channels. A more detailed discussion of HCN channel selectivity and the pore will follow (see Section C-a). HCN inward currents are blocked by cesium and are reduced in amplitude when the concentration of extracellular K^+ is reduced. Despite the high degree of homology among HCN channels, the different isoforms differ substantially from each other in some parameters, including the time constants of activation, the midpoint potential for channel activation, and the effects of modulation by cAMP.

i. Mammalian HCN channels

The time constants of activation among the mammalian HCN channels show a surprising diversity, considering their similarity in sequence. As recorded from HEK293 cells, the time constants for activation to a -100mV step are 67ms for HCN1, 562ms for HCN2, 1244ms for HCN3 and 5686ms for HCN4[20, 21]. Obviously, there is a dramatic slowing of the kinetics of activation from HCN1 to HCN4, going from a time scale of milliseconds to seconds. In addition, the midpoint potentials for channel activation ($V_{1/2}$) in mammalian HCN channels are -70.0 mV for HCN1, -96mV for HCN2, -77mV for HCN3, and -100mV for HCN4. The structural basis for the difference in kinetics is thought to be due to differences present in the S1-S2 linker and the cytoplasmic region of S6 [22]. There is only an 8 amino acid difference in the S1-S2 linker between HCN1 and HCN4. Exchanging single amino acids between HCN1 and HCN4 made very little difference in the kinetics of activation[22]. However, multiple point mutants had effects that were additive, slowing down the kinetics of HCN1 or speeding up the kinetics of HCN4 [22]. There was no significant change in the midpoint potential for channel activation. There was also no change in the kinetics of deactivation. A later study from the same group suggested that given the high homology in the core protein sequence in HCN channels, it is the peripheral domains of the N and C-termini that may play a role in giving rise to the differences in activation kinetics [23] Another group found that mutating a single leucine in the S1-S2 linker of HCN4 accelerated the kinetics of activation

to a level similar to HCN2[24], suggesting that differences in the S1-S2 linker may play an important role in the activation kinetics of HCN channels.

ii. Non-mammalian HCN channels

The non-mammalian HCN channel, spHCN1, has also been studied in order to help answer questions about the biophysical properties of HCN channels . Cloned from sea urchin sperm[18], spHCN1 shares much similarity with mammalian HCN channels. spHCN1 has a tetrameric structure with each subunit containing 6 transmembrane domains, a positively charged S4, and a GYG sequence in the pore loop. The currents of spHCN1 are similar to mammalian HCN channels, in that they are activated by hyperpolarization and have a sigmoidal waveform, are carried by Na^+ and K^+ , and are modulated by cyclic nucleotides. The midpoint potential of channel activation is -50mV for spHCN, much more positive than mammalian HCN channels. In addition, spHCN currents are very sensitive to the absence of cAMP, which cause spHCN currents to appear transient in nature[18]. The application of various concentrations of cAMP to excised patches increases spHCN1 currents in a dose dependent manner, with a $K_{1/2}$ of 0.74 μM [18]. Inward spHCN currents are also susceptible to a concentration and voltage dependent block by cesium and are drastically reduced in the absence of extracellular K^+ , just like in the mammalian HCN channels[18].

iii. cAMP modulation

Early on in the study of pacemaker currents, it was observed that application of cyclic-nucleotides regulates the rate of action potentials in the heart. Cholinergic stimulation shifts the voltage sensitivity of the pacemaker current to more negative voltages and causes a slowing of the diastolic depolarization, while β -adrenergic stimulation shifts the voltage sensitivity of pacemaker currents to more positive voltages and steepens the rate of diastolic depolarization[15, 25]. The mechanism of action for this autonomic regulation of pacemaker current was found to be caused by the direct interaction of cAMP with the CNBD domain of HCN channels, $K_d < 1\mu\text{M}$ [26].

All HCN channels have a cyclic-nucleotide binding domain, however the effects of application of cyclic-nucleotides to different isoforms of HCN channels have varied consequences. HCN1 is relatively insensitive to applied cAMP, since cAMP applied to inside-out membrane patches containing cloned HCN channels, produces only a +6mV shift in the midpoint potential of channel activation. HCN3 is also relatively insensitive to the application of cAMP. In contrast, HCN2 and HCN4 have robust responses to applied cAMP, with shifts of +25mV in their midpoints of activation. Furthermore, the kinetics of activation for HCN2 and HCN4 were increased 2 and 4 fold respectively (Steiber et al., 2005). A more detailed discussion of the CNBD domain will follow later (see Section C-b).

d. HCN channel expression in the body

HCN channels are expressed throughout the body, with different HCN isoforms specific for certain structures[15, 25]. All four HCN isoforms are expressed in the brain, with HCN3 having the lowest expression. HCN1 is expressed in layer V pyramidal neurons of the neocortex, CA1 pyramidal neurons, and inhibitory basket cells and purkinje neurons of the cerebellum. HCN2 and HCN4 are both found in the excitatory thalamocortical relay neurons, while only HCN2 is expressed in inhibitory thalamic reticular neurons[15, 25]. The I_h current from CA1 neurons is rapidly activating while the I_h current in thalamocortical relay neurons is slowly activating, reflecting the diversity of the HCN currents arising from differential HCN gene expression [27]. In the heart, where the I_f current was first discovered, HCN1, 2, and 4 are present. HCN4 is the predominant isoform in the SA node, as well as cardiac purkinje fibers. HCN2 is mainly found in the ventricles[15, 25]. The functional expression of I_f within the heart does not completely match HCN isoform localization. For example, the SA node I_f current does activate faster than one might expect for a region dominated by the slowly activating HCN4 isoform. This could be caused by a developmental change in the expression ratio of different HCN isoforms. It may also be a result of different subunits of HCN isoforms coassembling to form heteromers, or a result of some unidentified modulating factor

i. Subunit assembly

Evidence supporting the coassembly of different subunits comes from experiments where a co-injection was done for HCN1 and HCN2 RNA in

Xenopus oocytes. The resulting currents have properties that cannot be a result of the overall current from independent HCN1 and HCN2 homomers[28]. In fact these currents most resembled I_h in CA1 pyramidal neurons, suggesting that HCN channel coassemble in the body. Another experiment that supported coassembly of HCN channels, showed that a dominant-negative HCN2 pore mutant suppressed both HCN1 and HCN2 wild-type expression

e. Physiological role

HCN channels are proposed to have several physiological roles. The first and most well known is regulation of pacemaker activity in cardiac and neuronal cells. HCN channels mediate an inward current in the SA node, which prevents extreme hyperpolarization away from threshold, while simultaneously raising the cell potential to threshold, allowing other Na^+ and Ca^{2+} channels to activate[25].

HCN channels also play a role in dendritic integration. The expression of HCN1 channels in the dendrites of CA1 pyramidal neurons increases the more distal the dendrite is from the soma. HCN1 mediates an I_h current, which acts to normalize the distal EPSP's with proximal EPSP's[25], by increasing the resting membrane conductance at distal dendrites, decreasing the membrane time constant and accelerating the decay of the distal EPSP's.

HCN channels have been found in presynaptic terminals, including chick ciliary ganglion neurons, crayfish neuromuscular junction, and cerebellar basket cells. This suggests a role for HCN channels in synaptic transmission. The most compelling evidence for such a role comes from the experiment showing that block of I_h current with ZD7288 inhibited synaptic facilitation by serotonin[29]

i. Effects of HCN knock-out.

A HCN2 knock-out mouse has been made to gauge the physiological effects on a systemic level[30]. These mice were found to display cardiac sinus dysrhythmia and a reduction of the sino-atrial node HCN current. In addition, there was an increased susceptibility to oscillations in thalamocortical neurons, which caused an increase in the incidence of generalized absence epilepsy.

C. Structural bases for the functional properties of HCN channels

a. The pore domain of HCN channels

i. Permeation and Blocking properties

HCN channels are non-selective cation channels, despite having a GYG selectivity filter, conducting both Na^+ and K^+ but are impermeable to Li^+ [5]. They are slightly more selective for K^+ , having a $P_{\text{Na}}/P_{\text{K}}$ ranging from .25 to .41. As a result, their reversal potential is -30mV, between the reversal potentials for Na^+ and K^+ . HCN channels are neither permeable to divalent ions nor blocked by divalent ions, including Ba^{2+} , which blocks most other K^+ selective channels. However, one study found that a very low fraction of the HCN current was

actually carried by Ca^{2+} , $0.60 \pm 0.02\%$ [31]. HCN inward currents are blocked by extracellular cesium, at concentrations of 1-2mM [25], but for an unknown reason, the outward currents are potentiated by extracellular cesium. One selective blocker of HCN channels is ZD7288, a bradycardic agent that blocks mammalian HCN channels reversibly, but spHCN irreversibly. The difference in blocking characteristics for spHCN arise from the three non-adjacent residues (phenylalanine-x-leucine-x-isoleucine) lining the pore in the S6 region[32]. When these residues were substituted into HCN1, the ZD7288 block of HCN1 inward currents also became irreversible.

The inward current in HCN channels is also very sensitive to changes in the extracellular concentrations of K^+ and Cl^- . Decreasing the concentrations of K^+ ions will almost completely eliminate the Na^+ current, which is interesting because at physiological concentrations, most of the HCN current is carried by Na^+ . The dependency on K^+ ions may be due to Na^+ ions binding very tightly within the pore in the absence of K^+ [33], but a true structural explanation is still not known. Replacing Cl^- with large organic ions (such as isothionate and gluconate) will result in the almost complete loss of inward and outward currents through HCN2 and HCN4 channels[15]. The complete absence of extracellular Cl^- will decrease currents by 90% for HCN2 and HCN4 while only 10% for HCN1. The dependency on extracellular chloride is attributed to an arginine residue, adjacent to the N-terminus side of the GYG sequence in the pore region[34]. The arginine is only present on HCN2 and HCN4. Changes in

the concentration of extracellular Cl^- only affected the amplitude of currents, not the voltage dependence of activation or ion selectivity. It is unclear how Cl^- affects the HCN currents, but it was suggested that Cl^- may promote channel opening through some allosteric mechanism linked to the channel gate.

ii. Structure of the HCN pore

The unusual permeation properties of HCN channels is surprising considering the similarity the HCN pore structure has with the pore of K^+ selective voltage-gated channels, including the GYG motif that is the selectivity filter for K^+ ions[35]. This sequence of glycine-tyrosine-glycine lies within the pore loop, which is located between the S5 and S6 transmembrane domains. It has been found that the GYG sequence lines the inner pore of HCN channels as it does in K^+ channels, suggesting a similar pore structure but with different permeation properties[36]. It has been proposed that the reduced ion selectivity in HCN channels may be due to a greater degree of flexibility in the pore of HCN channels[37]. There are several amino acids that differ in the pore loop between HCN and Kv channels, which may enable the HCN pore to have less ion selectivity, but this has not been proven experimentally. The crystallization of the KcsA channel, (which is a tetrameric K^+ channel that only has two transmembrane domains and a pore loop in each subunit), was a major advance in understanding the structural basis for ion selectivity and conduction. The ability to create a functioning chimera where the Shaker pore domain was swapped with KcsA [38], validated KcsA as a legitimate model for the pore

structure of all K⁺ selective channels. The KcsA crystal structure (crystallized in the closed state) in conjunction with the MthK structure (crystallized in the open state) [39], prompted MacKinnon to propose that the bottom half of S6 acts as the intracellular gate in K⁺ channels, with a glycine in S6 acting as a hinge. Considering the functional differences between Kv channels and HCN channels, there is no reason to make the same assumption for the pore of HCN channels.

iii. HCN channels have an intracellular gate

In order to use KcsA or MthK as models for HCN, evidence for the existence of an intracellular gate in HCN channels would be needed. Evidence for an intracellular gate in HCN channels came from trapping experiments using ZD7288, a selective blocker for HCN channels. The ZD7288 block of spHCN and HCN1 only occurred when the blocker was added during hyperpolarizing steps. Furthermore, depolarizations of ZD7288-blocked HCN channels (after the application of ZD7288 during a hyperpolarized step) trapped ZD7288 in the channels, since no recovery of HCN currents was seen as long as the membranes were depolarized [32]. Once the membrane was hyperpolarized again, the currents recovered again. This recovery had the same time constant as simply stopping the perfusion of ZD7288 during a hyperpolarized step, suggesting the presence of an intracellular gate that can trap ZD7288 inside the channel. Another experiment tested the voltage-dependent accessibility of cysteine mutants in the pore of spHCN to intracellular Cd²⁺ in excised patches[40]. The binding rate was reduced during depolarized potentials and

increased during hyperpolarized potentials, suggesting the presence of an intracellular gate. Cd^{2+} could also be trapped within the pore similar to what had been seen previously for ZD7288. The presence of an intracellular gate in HCN channels gave confidence for using the KcsA crystal structure as a homology model for the pore domain of HCN channels. In the second work in my thesis we used the KcsA model for the pore of HCN2 channels to identify residues involved in Mg^{2+} binding (see chapter III).

b. The CNBD domain in HCN channels

The HCN channel family is gated by voltage and modulated by cyclic-nucleotides. The ability to bind cyclic-nucleotides is due to the presence of the CNBD at the C-terminus of HCN channels. The CNBD lies in the intracellular solution and is present on all four subunits of the HCN channel. The physiological implications for the CNBD domain have been explained earlier, but the manner in which the CNBD modulates HCN current will be explained in more detail in this section.

i. CNBD and HCN channel opening

Ever since the first recordings had identified the I_f current, it has been known that this current can be modulated by autonomic neurotransmitters. Sympathetic stimulation increased the rate of I_f depolarization which accelerated the heart rate, while parasympathetic stimulation decreased the rate of I_f depolarization, decelerating the heart rate[15, 25]. The first clues for cAMP mediating this

modulation came from the fact that β -adrenergic agonists increase heart rate by increasing cellular levels of cAMP[41]. Acetylcholine, on the other hand, acts to decrease heart rate by lowering cellular levels of cAMP. The observation that cAMP, even in the absence of MgATP, enhanced I_f channel opening in excised patches, seemed to suggest a direct interaction between cAMP and a site on the cytoplasmic surface of the channel underlying the I_f current[26]. Of course, this channel was later cloned and named HCN. The sequence revealed the presence of a CNBD in the cytoplasmic portion of the C-terminus which was connected to S6 by a structure called the C-helix. A subsequent study found that application of 100 μ m cAMP to excised patches expressing HCN2, greatly facilitated the opening of the channel, by shifting the $V_{1/2}$ by +17 mV[42]. This was in contrast to the small + 6 mV shift seen for HCN1. Clearly, cAMP was shifting the voltage dependence of activation, albeit at different levels for different HCN isoforms. Eliminating the C-helix portion of the channel removed any cAMP sensitivity for HCN1 and HCN2[43]. Eliminating the CNBD shifted the midpoint of activation by +24mV for HCN2 and +7mV for HCN1[16]. From this data, a mechanism was proposed where the CNBD acts as an inhibitor to channel gating, which is relieved by the binding of cAMP. The inhibitory action of the CNBD was thought to act on the pore through the C-linker. cAMP binding would cause a conformational change in the CNBD relieving any inhibitory action it had on the pore domain of the channel. The differences in cAMP sensitivity among HCN channels was found to be caused by the interaction between the C-linker domain and the core transmembrane

domain[43]. In fact, exchange of the CNBD domain alone had no effect on basal gating for HCN1 and HCN2. More information about the mechanism of action between the C-terminus and the core membrane protein came in the form of the HCN2 C-terminus crystal structure

ii. Answers from the HCN2 CNBD domain crystal structure

The crystal structure for the carboxy-terminal segment of HCN2[44], made up of a bound cAMP, the C-linker and the CNBD, provided an opportunity to finally view the molecular basis for how the CNBD was able to modulate HCN channel gating. The crystal structure showed a four-fold symmetry for the C-terminal regions of HCN2, mirroring the assumed symmetry of the transmembrane part of the subunits. The C-linker was made up of six α helices followed by the four α helices of the CNBD, which also contained a β -roll between the first and second α helix. cAMP binding between the β -roll and the C-linker is thought to be stabilized by electrostatic interactions and hydrogen bonding. Based on the crystal structure, a mechanism for cAMP binding was proposed where a conformational change first occurs in the CNBD, followed by the rearrangement of the tertiary structure of the C-linker α -helices[44]. This rearrangement causes one of the C-linker α -helices to move outward, away from the channel pore, removing the inhibition caused by the C-terminal region.

c. Voltage-dependent gating of HCN channels

HCN channels open with the opposite voltage dependence compared to Kv channels, despite having a very similar sequence to Kv channels. Kv channels

open in response to depolarization, while HCN channels open in response to hyperpolarization. An understanding of this reversed voltage activation of HCN channels is the main focus of this thesis. The study of HCN channels has the potential to reveal greater insights into the general function of the superfamily of voltage-gated ion channels, particularly the mechanism by which voltage-gated ion channels couple voltage sensitivity to changes in their conductance. The foundation for answering such questions lies in the research done by Curtis and Cole and Hodgkin and Huxley[1, 2] in the mid-twentieth century. The results from their work, which culminated in the ionic theory of membrane excitation, continue to echo throughout all structure-function research relating to voltage-gated ion channels, including HCN channels. Since voltage-gating is a central theme in this thesis, I will first describe the work by Hodgkin and Huxley, including the voltage-dependent gating mechanism in Kv channels, followed by brief overview of possible models for voltage activation in HCN channels.

i. Hodgkin and Huxley

Hodgkin and Huxley were concerned with the flow of electric current through the surface membrane of the squid giant axon. Their work was preceded by observations from Cole and Curtis showing a significant increase in membrane conductance that accompanied each action potential. Utilizing the newly developed voltage-clamp procedure, Hodgkin and Huxley were able to measure ionic currents flowing across the membrane. They identified two major

components to the ionic current, I_{Na^+} and I_{K^+} , which presumably passed through ion specific pores (channels) in the membranes. Hodgkin and Huxley next sought to develop a quantitative measure of the membrane ion permeabilities that gave rise to the total current in an action potential. They created a protocol that measured what they referred to as the “instantaneous current-voltage relation”, where a depolarization step was first applied to an axon to increase the permeability of the membrane, followed by steps to other voltage levels, where the current was then measured before any changes in permeability could occur [1, 45]. Using this protocol during predominantly Na^+ or K^+ permeability conditions, Hodgkin and Huxley defined the ionic conductances with two formulas.

$$g_{Na} = I_{Na}/(E-E_{Na}) \text{ and } g_K = I_K/(E-E_K)$$

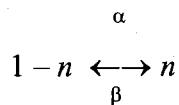
The conductance is represented by g , current by I , voltage step by E and reversal potential by E_K or E_{Na} . The conductance changes for Na^+ and K^+ were time and voltage dependent. A depolarization would cause the Na^+ conductance to rise quickly and then fall after a short period of time (ms), while the K^+ conductance would rise at a much slower rate, falling only when the depolarization step was terminated. Ion channels had not yet been cloned, so a molecular explanation for these conductance changes eluded Hodgkin and Huxley, however, they focused on developing a kinetic model to account for the shape and velocity of the action potential. The K^+ current, for instance, had a sigmoidal time course of activation following an initial delay, but an exponential deactivation. Hodgkin and Huxley found that this behavior could be

accounted for, using their conductance equations, if the K^+ channel was controlled by several independent gating “particles” embedded in the membrane and that the channels would open only when all gating particles were activated [1]. In this case, the probability that each particle is in the correct position to open a channel would be n and the probability for a tetrameric channel to be open would be n^4 .

The predicted particles would have an electric charge, allowing their position within the membrane to be voltage dependent. The movement of each particle to an activated vs deactivated state was presumed to be a first order reaction by Hodgkin and Huxley. Any change in voltage would thus change the probability of one particle being in either position exponentially to a new value[45]. The prediction of four such particles accounts for the sigmoidal activation curve of a K channel, resulting in the equation:

$$I_K = n^4 g_K (E - E_K)$$

The first-order reactions are represented by the equation,



One side of the equation represents the proportion of gating particles in the ‘open’ channel position ($1-n$), with the proportion of gating particles in the ‘closed’ channel position on the other side (n). α and β represent the voltage-dependent rate constants between the two positions of the gating particles. Solving the differential equation for this equation (knowing the initial value for the probability n) will predict the changes for a variety of axon potential

parameters [45]. Using the Hodgkin and Huxley model as a base, scientists have been able to understand and study the mechanisms underlying the action potentials in the nervous system.

ii. Gating particles and gating current

As ion channels were cloned, research into the structural basis of ion channel function began. One significant area of research was to identify the gating particles, predicted by Hodgkin and Huxley to control the opening and closing of the channel. The first K channel cloned was *Drosophila* Shaker[46]. Cloning and heterologous expression allowed for structure-function studies to identify the physical mechanisms behind the Hodgkin and Huxley theory of membrane excitation. As described earlier, the superstructure of voltage-gated channels included six transmembrane domains (S1-S6). A prime candidate for the gating particle, predicted by Hodgkin and Huxley, was the S4 domain, which included several positively charged amino acids (arginine or lysine) spaced at every third residue. Subsequent experiments showed the tetrameric structure of K channels[47], and therefore the presence of four S4 domains per channel, further making the case for S4 as the putative gating particle in a voltage gated ion channel. Changing the membrane electric field would therefore cause the movement of any charges that lay within the field (gating charges or voltage sensor), meaning a depolarization would move the charges outwards towards the extracellular solution, while a hyperpolarization would move the charges inwards, towards the intracellular solution. Such a movement of charge could

then be recorded as a small transient current, referred to as the gating current, which was first recorded in 1973 in Na channels[48]. Gating current was the nonlinear component of the membrane current that was seen when the ionic current was removed, by either a blocker or a mutation rendering the channel nonconducting. Gating currents represented the movement of a finite number of gating particles within channels. The amplitude of the gating currents is largest in the beginning of the voltage pulse when all channels are available to open, and decreases as fewer and fewer channels are left to open. Integrating the area under the gating currents gives the total gating charge. Essentially, changing the voltage caused a conformational change in the channel that moved a gating charge of valence, Z , across the membrane potential drop, E [45]. The increase in electrical energy caused by a membrane potential change is represented by a product of the valence, elementary charge, and membrane potential change: $-zqE$. W represents the steady state energy difference between open and closed states, so the total change in energy becomes $(w-zqE)$. A variation of the Boltzman equation produced an equation defining the voltage dependence of gating in terms of the fraction of open channels vs membrane potential for a two state model in which channels can either be open (O) or closed (C).

$$O/(O + C) = 1/(1 + \exp[(w-zqE)/K_bT])$$

K_b is the Boltzman constant and T is absolute temperature.

Essentially, the more charges that are moved in a channel by voltage, the steeper the voltage dependence of gating. Any changes in the gating charge would theoretically change the steepness or midpoint for the voltage dependence of

gating. The next step was the actual manipulation of charges in the S4 domain to see if these effects actually happened.

iii. S4 is the voltage sensor in Kv channels

The first experiment to mutate S4 charges was performed in Na channels, where basic amino acids in the S4 domain were changed to neutral residues[49]. As expected, removing the positively charged amino acids reduced the steepness of the voltage dependence of activation. Similar results were found for the S4 of Shaker channels, meaning that mutations of S4 changed the gating charge, suggesting the mutated segment of S4 must at least interact with parts of the channel that couple voltage to gating[50-52]. However, in order to make a comparison of gating charge before and after the mutation of an S4 charge, a method was needed to calculate the gating charge per channel, not just the total gating charge for all channels in a patch. Several methods were developed to count the number of channels present combined with the integration of the gating current[53], and produced a value of about 12 gating charges per Shaker K channel. This was followed by experiments correlating the removal of S4 charges to a decrease in the gating charge per channel[54]. Certain residues had more of an impact than others, providing an estimate of what portion of S4 truly acted as the gating charge. The caveat, was that in some cases, other mutations that conserved charge or swapped neutral residues could also change the voltage dependence of activation. To truly establish S4 as the voltage sensor, a method was needed to test for the voltage-dependent movement studies were developed

in which S4 charges were mutated into cysteines and tested for their accessibility to membrane impermeant cysteine reactive compounds such as MTSET (methanethiosulfonate-ethyltrimethylammonium). This method was called SCAM, (substituted-cysteine accessibility method), and was also used in the first paper included in this thesis (Chapter II) to show that S4 is the voltage sensor in a mammalian HCN channel. For Kv channels, SCAM was used to find that a section, including up to five charges in the Shaker S4, translocated across the membrane in response to changes in voltage [55]. The S4 was proposed to move outwards in response to a depolarization and inwards in response to a hyperpolarization. The movement of charge in the Shaker S4 could account for the gating charge after a depolarization step, indicating that the movement of S4 was the gating particle that had been predicted by Hodgkin and Huxley. Further research was needed, however, to find the mechanism by which the movement of S4 was translated into the opening and closing of the channel gate. It was during this time, that HCN channels were cloned and found to share the same structure as Kv channels, including a positively charged S4. However, for the HCN channel family, a depolarization step closed the channel gate while a hyperpolarization step opened the channel gate. This seemed highly unusual given the degree of homology between depolarization-activated channels and hyperpolarization-activated HCN channels. How could two homologous channels be activated by opposite voltages? For answers, people first looked to close relatives of HCN channels that had similar characteristics, such as gating

by hyperpolarization and inward rectification. Channels with these characteristics are Kir, HERG and KAT1 channels.

d. Models for HCN channel gating

HCN channels are first and foremost inward rectifiers. Other inward rectifiers are Kir, HERG and KAT1. Kir channels have only two transmembrane domains and are gated by the voltage dependent block from cytoplasmic factors. HERG and KAT1 are both more structurally similar to HCN channels. Despite their structural similarities, HERG and KAT1 have different molecular mechanisms that bring about their inward rectification. It was thought that one of these channels, (HERG or KAT1) would most likely provide a suitable model that could account for the inward rectification seen in HCN channels.

i. Kir model for HCN gating

Kir channels are inward rectifiers, like HCN channels, that also exhibit voltage-dependent gating, despite having only two transmembrane domains, the equivalent of S5-S6 in HCN channels, and much larger cytoplasmic N and C terminals. The molecular mechanism for gating in these channels was not caused by an intrinsic rectification found within the channel structure, but from cytoplasmic factors that are found in the intracellular solution of cells. These intrinsic rectifying factors were polyamines, (spermine, spermidine, putrescine, and cadaverine), which act to block the Kir channel pore in a steep voltage-dependent manner, in response to depolarized steps. The steepness increases

with polyamine positive charge and the affinity of channel block increases with polyamine chain length. Could this mechanism be applied to HCN channels? The results from the first paper, included in this thesis, would not support the Kir model. The first paper shows S4 as the voltage sensor, whose voltage-dependent movements are linked to channel opening. However, the second paper, included in this thesis, shows that Mg^{2+} can also cause some degree of inward rectification in HCN channels.

ii. HERG model for HCN gating: recovery from an inactivated state

HERG channels share a similar structure to depolarization-activated K^+ channels as well as HCN channels. In addition, it exhibits inwardly rectifying currents, like HCN channels. The mechanism that underlies the inward rectification in these channels are due to the time constants of HERG activation and inactivation. In HERG channels, the activation process is slow, but inactivation is fast. The result of such a kinetic scheme is that very little current is observed on depolarization, since the channels inactivate as soon as the channels open[15]. Depolarization is still required for the channels to open in the first place, but the channels quickly enter a C-type like inactivated state in which no current is passed. The channels quickly recover from inactivation at hyperpolarized potentials, producing an inward current that closes slowly. An experiment where the HERG channel was activated by a depolarized step followed by a hyperpolarized step, and then depolarized again before the channels had fully closed, revealed the presence of large outward currents[56]

and a subsequent linear I-V. This seemed to suggest that the inward rectification seen in HERG channels was dependent on the kinetics of the inactivation process. This was confirmed by a mutation which completely eliminated HERG inactivation, producing a HERG channel that had no inward rectification. HCN channels, however, with the exception of spHCN(which is thought to be gated by voltage and cAMP), show no such inactivation. A modification of the HERG model could potentially accommodate the behavior of HCN and spHCN channels, based on the results from three point mutants on the Shaker S4[57]. These mutants shifted the midpoint of activation to very negative potentials. Inactivation remained intact in Shaker, so the channels were nonconducting at the resting potential. Hyperpolarized steps caused a recovery from inactivation and produced inward currents that did not close due to the very negative midpoint of activation for these mutant Shaker channels. These currents are very similar to the currents through HCN channels. The inward rectification in HCN channels, however, are a direct result of the voltage-dependent movement of S4, which opens and closes the gate. The same is true for spHCN, however it does show inactivation, though this is caused by low levels of cAMP which allows the CNBD to inhibit the opening of the channel. Application of cAMP to an excised patch expressing spHCN channels, will eliminate the inactivation process.

iii. KAT1 model for HCN gating: activation from a closed state

An alternative model proposes that gating in HCN channels is a result of the direct movement of S4, but oppositely coupled to the activation of the channel compared to Kv channels. This model had been suggested for KAT1[58]. KAT1, like HCN1, activates with a sigmoidal time course and shows no inactivation once the channel has opened. Mutating charged KAT1 S4 residues caused a positive shift in the voltage dependence of activation[58]. The shift was in the same direction seen for similar mutations in the depolarization-activated Shaker channel. In addition, one of the S4 mutants, where a charged residue was replaced by neutral amino acid, caused a decrease in the slope value (Z) for the Boltzman fit of the plot of voltage dependence vs open probability. These results suggested that S4, as in Shaker channels. acts as the voltage sensor, undergoing a conformational change in response to a change in voltage. The positive shift caused by mutating charged S4 residues, also suggests that the movement of S4 in KAT1 is similar to that of S4 in Shaker channels, albeit with a reversed coupling mechanism to the channel gate. These studies provided further evidence for S4 as the voltage sensor but did not show direct evidence for voltage-dependent conformational changes in S4. Direct evidence for the voltage-dependent movement of S4 is included in the first paper of this thesis.

iv Early structure/function studies of HCN S4

If a KAT/Shaker like model is applied to HCN channels, it is interesting to note the differences in the S4 domain between HCN/KAT1 channels and the Shaker S4. The S4 domain in HCN/KAT1 channels is larger, containing eight to ten

positive charges every third residue as opposed to the five or seven charges, also spaced every third residue, found in depolarization activated channels. The presence of a serine, in place of a charged residue found in Kv channels, within the S4 domain in HCN/KAT1 channels is another key difference. The functional role for this serine is unknown. One study attempted to define the roles of the charged residues in HCN2 by mutating all nine positive charges on the S4 domain[59]. As in a previous HCN2 S4 study[60], mutation of the N-terminus S4 charges caused a left shift in the midpoint of activation, potentially implicating these residues as surface charges, with only limited roles in voltage-dependent gating. The role of a surface charge would be to screen S4 from excess negative residues on the protein surface that could potentially influence the energetics of S4 conformational changes. Evidence from this study showing that these charges can act as surface charges is the finding that mutating all four S4 N-terminus charges dramatically shifted the voltage dependence of activation. The addition of extracellular Mg^{2+} reversed this shift by up to +20mV [59]. Mutation of charges in the middle portion of the S4 domain, in addition to the serine, reduced current amplitude, while mutation of charges towards the C-terminus resulted in non-expressing channels, implicating these residues as important for gating in HCN channels. An additional finding from this study, was the loss of channel function when mutating, individually, two negative charges in S2 and two negative charges in S3. In Shaker, the homologous residues are thought to have electrostatic interactions with the middle portion of S4 [61, 62]. Though no studies to examine interactions between S2-S3 and S4

have been done for HCN channels, the fact that they are essential for HCN channel function may suggest a similar orientation of S4 towards other portions of the channel as in Shaker. The experimental evidence for potential interactions between S4 and S2-S3 in Shaker, suggested that the S1-S4 may undergo a collective conformational change to move gating current. S1-S4 were referred to as the voltage-sensing domain, with S5-S6 as the pore domain.

v. Coupling between S4 and the channel gate

The obvious structural link between the two is the S4-S5 linker in the intracellular matrix which could potentially couple the S4 to the channel gate in the pore domain. Mutations in the S4-S5 domain had been found to cause changes in the voltage dependence and kinetics of activation gating in Shaker, Kv2, Kv3, and HERG[63-65]. A similar study was done for HCN2, where an alanine scan was performed on the S4-S5 linker[66]. Three residues were found to disrupt channel closing, suggesting the S4-S5 linker as the coupling mechanism between S4 and the channel gate. More experimental evidence, however, is needed to further distinguish these effects as a direct action on coupling versus a 'downstream' effect in the protein apparatus.

vi. Crystal Structures

No discussion of voltage-dependent gating would be complete without considering the implications from crystal structures, especially the more recent KvAP and Kv1.2, which both have a similar structure to voltage gated K⁺

channels. Crystal structures provide a static view of one protein conformational state, but are invaluable in directly observing the relationship between different parts of the protein. Just as KcsA and MthK provided information about the pore domain, KVAP and Kv1.2 have provided some insight into the structure of the voltage-sensing domain[67-69] The structure for KVAP suggested a structure where the pore was surrounded by voltage sensors in the form of 'paddles'. The paddles are made up of the N-terminus portion of S3 and the S4 forming a helix-turn-helix structure that moves through the membrane in response to voltage. This structure was greeted with skepticism due to concerns about the energetics of positive charges moving through the lipid membrane. Subsequent work refined this model of S3-S4 movement to include more of a vertical rotation, similar to what was proposed for the S4 domain in Kv1.2. The Kv1.2 crystal structure suggested a relatively independent S4 domain within the membrane that acted via the S4-S5 linker to constrict or dilate the S6 inner helices. Evidence for an independently acting S4 domain comes from previous experiments transferring the S1-S4 of Shaker to a KcaA channel, producing a voltage-dependent gating channel. The S4 domains of Kv1.2 seemed to 'float' at the corners of the pore, lacking any substantial contact with the pore. Similar to KcsA, the S4-S5 linker translates the motion of S4 into a constriction or dilation of the inner helices of S6. Results from the first paper (Chapter II), included in this thesis, do not support such a large movement of charge within the membrane as first suggested for KvAP. Instead, the middle portion of S4 moves completely across the membrane as HCN1 goes from a closed state to an

open state. The four charges at the N-terminus of S4 did not show any state-dependent accessibility changes, suggesting that these charges are always exposed to the extracellular solution, and do not move through the membrane in response to changes in voltage. This does not rule out a conformational change for the N-terminus S4, but any movement that occurs probably does not traverse the transmembrane electric field.

vii. Future Directions for HCN study

The two major conclusions from this thesis are 1) S4 is the voltage sensor in mammalian HCN channels. The voltage-dependent movement of S4 is coupled to the opening and closing of the channel gate causing inward rectification. 2) Mammalian HCN channels are also susceptible to an inward rectification caused by intracellular Mg^{2+} which blocks outward currents in HCN channels.

These results are essential first steps in understanding the mechanism by which the movement of S4 is coupled to the channel gate. The fact that HCN channels are so structurally similar to Kv channels means that any advances in the understanding of coupling in Kv channels will most likely provide some degree of insight into the function of HCN channels and vice versa. The existence of crystal structures for Kv channels does provide a creative foundation for future experiments on the voltage-sensing domain just as KcsA invigorated the study of the pore domain. An HCN crystal structure would be most helpful in gaining insight into the relationship between the voltage-sensing domain and the pore

domain, but until then, further insights will progress in small but meaningful steps that may ultimately create a comprehensive model for HCN channel gating.

II. Chapter 2

S4 movement in a mammalian HCN channel

Sriharsha Vemana, Shilpi Pandey, and H. Peter Larsson

Neurological Sciences Institute, Oregon Health & Science University
505 NW 185th Avenue, Beaverton, OR 97006

Corresponding Author: H. Peter Larsson

larssonp@ohsu.edu

Phone: 503-418-2655

Fax: 503-418-2501

E-mail: larssonp@ohsu.edu

Running Title: S4 movement in HCN1

Keywords: voltage sensor
hyperpolarization-activated
cysteine accessibility
SPIH

Acknowledgements

We thank Drs. Fredrik Elinder and Hans Koch for comments and suggestions; and Sandra Oster for editing the manuscript. This study was supported by a grant from NIH (NS043259) to HPL.

A. Abstract

Hyperpolarization-activated, cyclic nucleotide-gated ion channels (HCN) mediate an inward cation current that contributes to spontaneous rhythmic firing activity in the heart and the brain. HCN channels share sequence homology with depolarization-activated Kv channels, including six transmembrane domains and a positively charged S4 segment. S4 has been shown to function as the voltage sensor and to undergo a voltage-dependent movement in the Shaker K⁺ channel (a Kv channel) and in the spHCN channel (an HCN channel from sea urchin). However, it is still unknown whether S4 undergoes a similar movement in mammalian HCN channels. In this study, we used cysteine accessibility to determine whether there is voltage-dependent S4 movement in a mammalian HCN1 channel. Six cysteine mutations (R247C, T249C, I251C, S253C, L254C, and S261C) were used to assess S4 movement of the heterologously expressed HCN1 channel in *Xenopus* oocytes. We found a state-dependent accessibility for four S4 residues: T249C and S253C from the extracellular solution, and L254C and S261C from the internal solution. We conclude that S4 moves in a voltage-dependent manner in HCN1 channels, similar to its movement in the spHCN channel. This S4 movement suggests that the role of S4 as a voltage sensor is conserved in HCN channels. In addition, to determine the reason for the different cAMP modulation and the different voltage range of activation in spHCN channels compared to in HCN1 channels, we constructed a C-terminal-deleted spHCN. This channel appeared to be similar to a C-terminal-deleted HCN1 channel, suggesting that the main

functional differences between spHCN and HCN1 channels are due to differences in their C-termini or in the interaction between the C-terminus and the rest of the channel protein in spHCN channels compared to in HCN1 channels.

B. Introduction

HCN channels are members of the super family of voltage-gated ion channels and are activated by membrane hyperpolarization[15, 25]. The opening of the channel generates an inward current that raises the membrane potential of a cell towards threshold. This inward current enables HCN channels to regulate rhythmic activity in cells such as “pacemaker” cells in the heart or neurons in the thalamus. HCN channels share the greatest sequence homology with depolarization-activated Kv channels [15, 25]. Both HCN and Kv channels are tetramers, with each subunit containing six transmembrane segments, a positively charged S4 segment, a pore loop between S5 and S6, and a GYG sequence motif in the selectivity filter (Fig. 2A). However, HCN channels, unlike Kv channels, possess a cyclic-nucleotide binding domain at the C-terminus, which allows intracellular, second-messenger molecules, like cAMP or cGMP, to modulate the activity of HCN channels[25].

The S4 domain in voltage-gated ion channels contains positive charges spaced at every third residue and is the most conserved domain among voltage-gated ion channels. S4 was early on hypothesized to be the voltage sensor in voltage-gated ion channels. S4 is relatively conserved between the depolarization-activated Kv channels and the hyperpolarization-activated HCN channels (Fig. 2A). Shaker K⁺ channels have seven basic residues in the S4 domain. Mammalian HCN channels have nine basic residues, spaced at every third residue within S4. A neutral serine residue divides these nine residues into two

groups, one of 4 and one of 5 (Fig. 2A). The spHCN channels have eight basic residues that a neutral serine divides into two groups of 4. Despite similarities between HCN and Kv channels, HCN channels open by hyperpolarizing potentials and close by depolarizing potentials, in contrast to Kv channels, which open during depolarizations and close by hyperpolarizations.

The difference in voltage dependence between HCN and Kv channels is even more intriguing in the context of recent findings showing that S4 in the sea urchin sperm clone (spHCN) and S4 in a bacterial HCN channel (MVP) move in a manner similar to the movement of S4 in depolarization-activated Kv channels (Shaker) [70, 71]. Previous studies have shown S4 to be the voltage sensor in Shaker K⁺ channels [54, 55, 72-74], where S4 moves outward during depolarization and channel opening, and inward during hyperpolarization and channel closing [55, 72]. S4 in spHCN channels has a similar movement, except that in these channels, inward movement opens the channels and outward movement closes them [70].

spHCN channels are one of several types of cloned HCN channels, including several cloned from mammalian sources (mouse, human, rat, and rabbit) [16, 18]. There are many functional differences among the HCN channel clones, but especially significant are those differences between mammalian HCN (HCN1-4) channels and spHCN channels. Mammalian HCN channels activate at more hyperpolarized potentials than spHCN channels [16, 18]. In addition, cAMP

shifts the voltage dependence of activation in mammalian HCN channels to more depolarized potentials, while cAMP increases the amplitude of currents through spHCN channels and removes a time-dependent inactivation that is present at low cAMP concentrations[16, 18].

Previous investigations into the role of the S4 domain in mammalian HCN channels involved mutating basic residues in the S4 of the HCN2 channel to neutral amino acids [59, 60]. The neutralization of basic residues in S4 resulted in a shift of the voltage-dependent activation to more hyperpolarizing potentials. These findings are significant in highlighting the importance of S4 in mammalian HCN channels. However, S4 movement in mammalian HCN channels has not been shown. The focus of our study was to utilize cysteine accessibility methods[70] to measure whether S4 in mammalian HCN1 channels moves during changes in membrane potential and whether S4 functions similarly to the voltage sensor in spHCN channels.

C. Methods

The experiments were performed on the mouse HCN1 channel and the sea urchin spHCN channel expressed in *Xenopus* oocytes. It has been shown that the endogenous cysteine C318 in HCN1 channels is extracellularly accessible to MTS reagents [75]. In our experiments, C318 was mutated to a serine, producing HCN1 channels with currents that were not modified by the extracellular application of MTSET (methanethiosulfonate ethyltrimethylammonium). The C318S mutation was subsequently used as a background HCN1 channel in which all cysteine mutations were made. In addition, to remove 6 of the intracellularly located cysteines and to eliminate the potential influence of cyclic nucleotides on the voltage dependence of HCN1 channels, the channels used in this study had the cyclic-nucleotide binding site domain removed by introducing a stop codon at residue S391 [42]. Similarly, we created a C-terminal-deleted spHCN channel, spHCN_{ΔC-term}, by introducing a stop codon at the corresponding site S472 in the spHCN channel.

a. molecular biology

Site-directed mutagenesis was performed on C318S HCN1 channels using the QuikChange Kit (Stratagene, La Jolla, CA). Initially, only charged residues were mutated to cysteines because it is the movement of charged residues that is most important in studying a voltage-gated ion channel. Lack of expression (see methods/molecular biology, Fig. 2A) of several of these charged residues led us to mutate adjacent, non-charged residues in order to test for voltage

dependent S4 movement (Fig. 2A). Residue K256 was excluded from our study due to the lack of expression that K256 mutants have exhibited in earlier studies [59, 60, 70, 76, 77]. The plasmid was linearized with Nhe1. RNA was synthesized *in vitro* using the T7 mMessage mMachine kit (Ambion, Austin TX) and injected (50nl of 0.1-1ng/nl) into *Xenopus* oocytes. The electrophysiology experiments were performed 2 to 6 days after the injection of mRNA. The lack of expression for a mutant was defined as no currents in a two-electrode voltage clamp from at least 3 different RNA injections and at least 2 different clones.

b. Electrophysiology

Cysteine-substituted mutant channels expressed in *Xenopus* oocytes were recorded with the two-electrode voltage clamp technique for extracellular accessibility studies and the patch-clamp technique for the intracellular accessibility studies. Microelectrodes were made from borosilicate glass and filled with a 3M KCl solution for the two-electrode experiments. Each electrode had a resistance of 0.5 to 1.0 M Ω . All experiments were performed at room temperature.

c. Two-electrode voltage-clamp technique.

Whole-cell ion currents were measured with the two-electrode voltage-clamp technique, using a CA-1B amplifier (Dagan Corp.). The bath solution consisted of a 100-K solution (in mM): 89 KCl, 15 Hepes, 0.4 CaCl₂, and 0.8 MgCl₂.

KOH was added to adjust the pH to 7.4, yielding a final K^+ concentration of 100 mM. The use of the 100-K solution produced larger amplitude currents, which allowed for better monitoring of current changes at the negative voltage pulse. During the recording of R247C, the bath solution consisted of a 1-K solution of (in mM): 1 KCl, 88 NaCl, 15 Hepes, 0.4 $CaCl_2$, and 0.8 $MgCl_2$. The pH was adjusted to 7.4 by the addition of NaOH. The use of the 1-K solution allowed for monitoring of changes in the tail currents at 0 mV, a potential that reduced the effects of contaminating leak currents.

d. Patch voltage-clamp technique.

The macro-patch currents were measured with the patch-clamp technique (Axopatch 200B, Axon Instruments). The extracellular pipette solution consisted of a 100-K solution (described above) and 1 mM $BaCl_2$ to block endogenous, single K^+ -channel events. The intracellular patch solution consisted of (in mM): 98 KCl, 0.5 $MgCl_2$, 0.1 $CaCl_2$, 1 EGTA, 10 Hepes, and 1 ATP. KOH was used to adjust the pH to 7.1.

e. Cysteine Labeling and Accessibility Studies

Cysteine residues were substituted, one at a time, for seven residues in the HCN1 S4 domain (Fig. 2A). Cysteine residues react with MTS reagents much faster ($>10^6$) in an aqueous environment than in an hydrophobic environment [78]; thus, the modification rate of a cysteine by a MTS reagent depends on whether the cysteine is located in the extra- or intracellular solution, or is buried

in the membrane. Changes in the accessibility of cysteine residues were tested by measuring the voltage dependence of the rate of irreversible covalent modification with the cysteine-specific compounds MTSET and MTSEA (methanethiosulfonate-ethylammonium). The MTS reagents (100 μ M to 2 mM) were dissolved in a 100-K solution and kept on ice until they were applied to the bath. A new MTS solution was made every 4 hours. A gravity-driven perfusion system was used in the application and the wash-out of MTS reagents. The time constant for the solution exchange was approximately 1 second (tested by applying 0.2 mM CsCl₂, which blocks approximately 50% of the HCN1 channels). The fast solution exchange ensured that the 10-second application and 20-second wash-out times were adequate enough to expose the oocyte to MTSET only at the desired potential. The MTS modification of the cysteine was monitored by a change in the current amplitude of the channel at a specific test voltage. This test voltage was chosen from a comparison of current/voltage plots before and after application of MTS reagents (see next section). Cysteine mutations that did not display any change in the current during the MTS treatment were not used to draw conclusions about cysteine accessibility.

A two-electrode voltage clamp was used to test for the extracellular accessibility of cysteines to MTSET. The patch-clamp technique was used to test for intracellular accessibility of cysteines to MTSEA that was applied to the cytosolic face of inside-out patches. A comparison of current/voltage curves before and after MTS application allowed us to determine the ideal test voltage

for each residue, that is, the voltage at which the difference in current amplitude is maximal between pre- and post-MTS application.

The extracellular modification protocol started at a holding potential of 0 mV, followed by a 200-ms step to the ideal test voltage determined for the residue (for example -120 mV for S253C). This voltage step was followed by a step to $+50$ mV, and in turn by a 30s step to either 0 mV or -100 mV. The application of MTSET occurred during the first 10 seconds of the 30-second step. The extracellular solution was perfused for the last 20 seconds to wash away any unbound MTSET.

The intracellular accessibility of the introduced cysteines was tested using MTSEA because the application of MTSET consistently destroyed the excised patches clamped to the very hyperpolarized voltage steps ($-120/-140$ mV) that were needed to open the HCN1 channels. A similar effect has been reported for patch clamp experiments using very negative potentials and MTSET on excised patches containing Shaker K channels [72, 79]. However, this effect was not seen with MTSEA. In addition, run-down was significant upon excising the patch[59]. The run-down was seen in all excised patch experiments; 5 minutes after patch excision, the current in response to a voltage step to -130 mV was reduced by $57\% \pm 7.5\%$. Therefore, to minimize the effect of run-down, we excised the patches directly into a bath solution containing $100 \mu\text{M}$ MTSEA for L254C and $200 \mu\text{M}$ MTSEA for S261C. We tested the state-dependence of

internal cysteine accessibility by applying different voltage protocols while the cytosolic face of the patch was exposed to the MTSEA bath solution. The closed state accessibility was tested using a 200-ms test pulse every 10 seconds from a holding potential of 0 mV (>90% of the time spent at 0 mV). Open state accessibility was tested using a 1-second hyperpolarizing voltage pulse every 2 seconds from a holding potential of 0 mV (50% of the time spent at hyperpolarized potentials). In some experiments, 20 mM cysteine was included in the pipette solution to scavenge MTSEA that diffused across the patch membrane [78, 80]. The addition of the 20 mM cysteine in the pipette solution did not alter the modification rates, indicating that the MTSEA modification was intracellular.

These protocols allowed us to measure the time course of modification with changes in the amplitude of the current plotted against exposure time (time [s] x concentration MTSET [mM]). From these plots, a mono-exponential curve was fitted and a pseudo first-order modification rate constant, k , was calculated from the time constant, $k = 1/\tau$ [$\text{mM}^{-1} \text{s}^{-1}$]. The potential used to test for open-state accessibility was more negative for internal accessibility than for external accessibility because the $G(V)$ shifts to more negative potentials after patch excision.

f. MTS Reagent Stability

An important consideration in using MTS reagents is their stability during the cysteine accessibility experiments. Ideally, solutions should be made immediately before their use in experiments. However, MTS reagents in solutions maintained on ice have been shown to be relatively stable for several hours [81]. We repeated an assay developed by Stauffer and Karlin (1994) to determine the half-times for hydrolysis of MTS reagents both in the solution used for this paper, i.e., 100-K solution (see above), as well as the solution used by Stauffer and Karlin, i.e., NP100; (100 mM NaCl, 10 mM NaPO₄, 1 mM EDTA, 3 mM NaN₃, pH 7.0). The assay tests for the formation of a mixed disulfide bond between the methanethiosulfonate reactive group and 5-thio-2-nitrobenzoate (TNB). 100 μM TNB was formed from the reaction of 50 μM DTT with 2 mM DTNB {5,5'-Dithiobis(2-nitrobenzoate)} [81]. TNB has a maximum absorbance at 412 nm [81]. The reaction of TNB with a MTS reagent causes a decrease in absorbance, thus allowing a quantitative measure of the non-hydrolyzed MTSET concentration in a solution. Initially, we measured the absorbance at 412 nm of 100 μM TNB with varying concentrations of MTSET dissolved in the 100-K solution in a quartz cuvette to generate a standard linear curve (Fig. 1A). Next, the stability of MTSET on ice or at room temperature was tested. MTSET was dissolved in a 100-K solution, in a NP100 solution, or in dH₂O that was kept on ice or at room temperature. At various time points from 0 to 500 minutes, 100 μl of MTSET was taken from the 100-K solution or the NP100 solution, and was added to the TNB solution for a final MTSET concentration of 50 μM. 50 μM was used because it was in the middle of the

linear plot shown in Fig. 1A. The absorbance of the MTSET/TNB solutions from the various time points were used, together with the standard curve (Fig. 1A), to calculate the remaining non-hydrolyzed MTSET concentration after incubation on ice or at room temperature (Fig. 1B). The results from this assay show that MTSET (even at physiological pH) maintained on ice was stable for at least 4 hours, the maximum duration of our experiments. It is interesting that MTSET in our 100-K solution at room temperature had a half-life of two hours, while MTSET in NP100 at room temperature had a much faster decay rate ($t_{1/2} = 13$ minutes). This faster rate of hydrolysis in NP100 is partly due to the presence of sodium azide in the NP100 solution, which accelerated the decay of MTSET (data not shown). The results from this assay show that MTSET hydrolysis was not a detrimental factor during the experiments reported here.

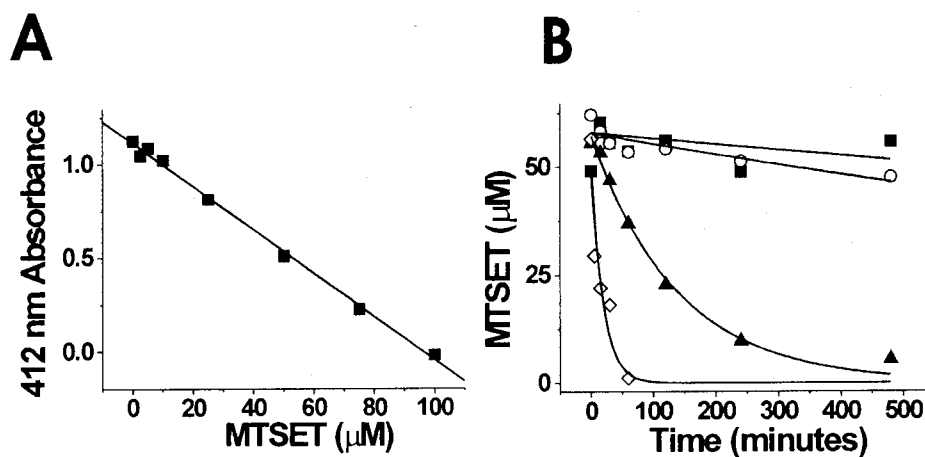


Figure 1. Stability of MTSET at room temperature and on ice. (A) Absorbance at 412 nm of 100 μM TNB dissolved in the 100-K solution containing different concentrations (0-100 μM) of MTSET. (B) A plot comparing the stability of MTSET over time in different solutions and at different temperatures. (■) MTSET in 100-K solution on ice, $\tau = 1420 \pm 312$ min; (○) MTSET in dH_2O on ice, $\tau = 4113 \pm 3000$ min; (▲) MTSET in 100-K solution at room temperature, $\tau = 111 \pm 8$ min; and (◇) MTSET in NP100 solution at room temperature, $\tau = 19.4 \pm 6.6$ min.

D. Results

a. S4 is the voltage sensor for HCN1

To test for S4 movement in HCN1 channels, we introduced cysteines at eleven residues in the S4 domain, one at a time (Fig. 2A), to determine the accessibility of the cysteine mutants to the MTS reagents applied in the extracellular and intracellular solutions. Of the eleven mutations, K250C, L252C, L258C, R259C, and L260C did not express. Figure 2B shows HCN1 currents from the HCN1 C318S mutant used as the background (see Methods and Materials), and Fig. 2C shows the conductance-versus-voltage curve, $G(V)$, for the expressing mutations.

The S4 domain is relatively well-conserved among HCN1, spHCN, and Shaker K^+ channels (Fig. 2A). Earlier studies have shown that cysteines introduced at positions 338 in spHCN channels and 368 in Shaker K^+ channels were accessible to MTSET from the intracellular solution at hyperpolarized potentials and from the extracellular solution at depolarized potentials, suggesting a complete transmembrane movement of these residues [55, 70, 72]. Therefore, we initially focused on the corresponding residue 253 in HCN1 channels to determine whether this residue has a similar, voltage-dependent transmembrane movement.

Table 1. Modification rate constants for mutants R247C, T249C, I251C, S253C, and L254C.

Cysteine Mutation	Extracellular Modification ($M^{-1}s^{-1}$)		Intracellular Modification ($M^{-1}s^{-1}$)	
	-100 mV	0 mV	-120/-140 mV	0 mV
R247C	350±60 (n=3)	650±280 (n=3)	Poor Expression	
T249C	2.9±1.0 (n=4)	13.5±4.5 (n=3)	Poor Expression	
I251C	No Effect (n=9)		Poor Expression	
S253C	1.2±0.24 (n=3)	9.2±1.6 (n=5)	Poor Expression	
L254C	No Effect (n=3)		1,540±420 (n=6)	<10 (n=6)
S261C	Not Tested		151±9 (n=3)	<10 (n=5)

Values given as mean ± SEM (n). k is the second-order rate constant for MTS modification of the specified channels at the indicated potentials. “No Effect” means that 1 mM MTSET for 2 minutes affected the current by less than 10%; thus, $k < 1 \text{ s}^{-1}M^{-1}$.

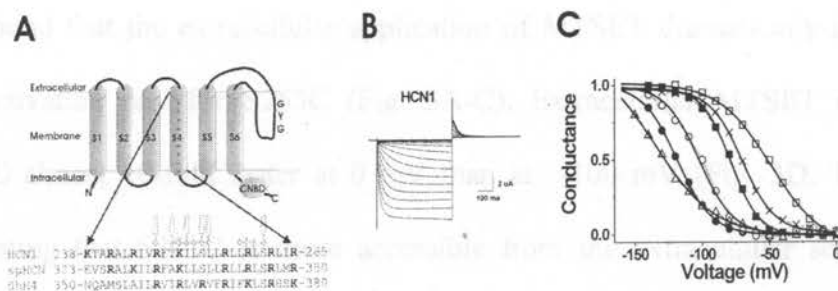


Figure 2. Membrane topology and sequence alignment of HCN1 channels.

(A) Above, membrane topology of the HCN1 channel, including six transmembrane domains (S1-S6), the cyclic-nucleotide binding site (CNBD), and the GYG K^+ selectivity sequence in the pore domain. Below, a sequence alignment between the S4 region of the HCN1, spHCN, and Shaker K^+ channels [18, 70]. The positively charged residues are in bold. The stars above the HCN1 channel note residues mutated into cysteines in this study. The arrows indicate mutations that expressed in oocytes: R247C, T249C, I251C, S253C, L254C, and S261C. (B) HCN1 currents elicited by voltage steps in -10 mV increments from 0 mV to -190 mV, from a holding potential of 0 mV, followed by a step to +50 mV for tail currents. (C) Representative G(V) curves from isochronal tails at +50 mV for the expressing mutations: (o) R247C, (●) T249C, (□) S253C, (■) L254C, (Δ) S261C, and the background channel (x) C318S.

We found that the extracellular application of MTSET dramatically increased the activation rate for S253C (Fig. 3A-C). Extracellular MTSET modified S253C almost 10-fold faster at 0 mV than at -100 mV (Fig. 3D, Table 1), suggesting that S253C is more accessible from the extracellular solution at depolarized potentials than at hyperpolarizing potentials. This state-dependence is similar to that which was found for S338C in spHCN channels.

We next attempted to test the state-dependence of intracellular accessibility for S253C to determine whether it also was similar to the state dependence of S338C in spHCN channels. However, in excised patches, S253C failed to express sufficiently to be tested for intracellular accessibility to MTS reagents. Channels with a cysteine mutant at the neighboring residue L254C, however, expressed at high-enough levels to detect current changes in excised patches. MTSET, in combination with hyperpolarizing steps to activate HCN1 currents, was found to be detrimental to patch stability, prompting the use of MTSEA instead (see Methods and Materials). At 0 mV and -120 mV (Fig. 4A-D), the intracellular application of 100 μ M MTSEA onto HCN1 C318S channels (used as our control) caused no significant changes in current amplitudes or current kinetics beyond the normal run-down associated with patch excision (see Material and Methods section and Chen et al., 2001). In contrast to this control recording, the intracellular application of MTSEA eliminated the voltage dependence of L254C currents (Fig. 4E-G), similar to the effects from the intracellular application of MTSET in the spHCN channel residues S338C and

L340C [70]. The intracellular application of MTSEA modified L254C much faster at -120 mV than at 0 mV (Fig. 4H, Table 1), which is opposite result to the voltage dependence seen from the extracellular application of MTSET on S253C. This finding suggests that L254C is more accessible from the intracellular side of the membrane at hyperpolarizing potentials than at depolarizing potentials. The extracellular application of MTSET and MTSEA had no effect on L254C, suggesting that L254C was never exposed to the extracellular solution. These findings of extracellular accessibility from S253C and extracellular/intracellular accessibility from L254C point to a transmembrane movement of the middle portion of S4 at residues 253 and 254.

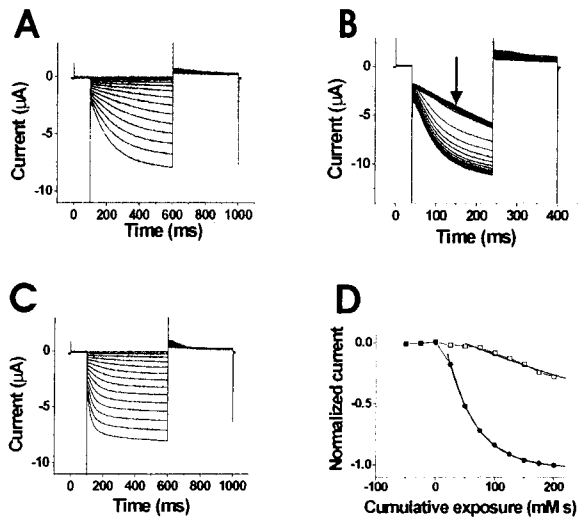


Figure 3. State-dependent accessibility of S253C. Currents before (A), during (B), and after (C) the application of 100 μM extracellular MTSET. In (A) and (C), the voltage steps are in -10 mV increments from 0 mV to -150 mV. In (B), voltage was held at 0 mV and then stepped to -120 mV for the test pulse, followed by a step to +50 mV for tail currents. The holding potential was 0 mV. MTSET was applied for 10 seconds during each episode. (D) Currents measured at the arrow in (B) as a function of cumulative exposure to MTSET. The modification time course for the extracellular application of 100 μM MTSET at 0 mV (\bullet) and at -100 mV (\square). The bold lines are an exponential fit to the data.

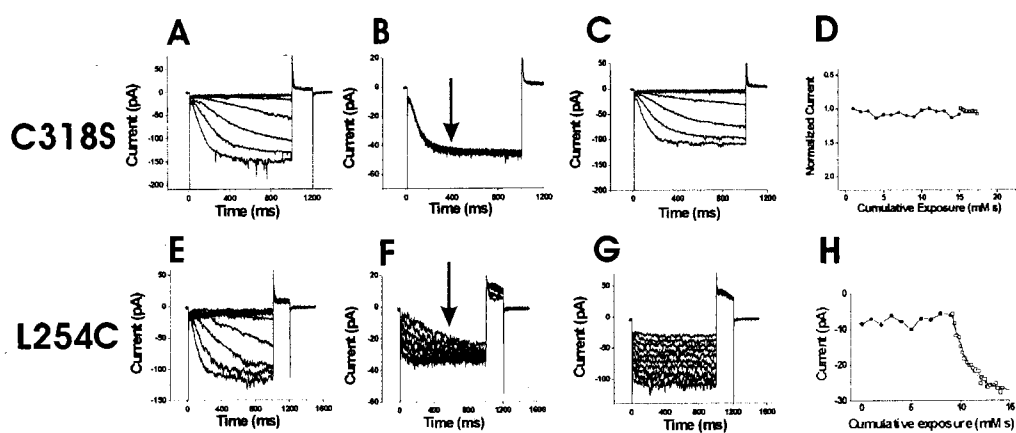


Figure 4. State-dependent accessibility of L254C. (A-D) Application of MTSEA on the background channel HCN1 C318S. Currents before (A), during (B), and after (C), the intracellular application of MTSEA onto inside-out patches expressing HCN1 C318S mutants. In (A) and (C) the voltage steps occur in -10 mV increments from 0 mV to -120 mV. In (B), the current trace is from a voltage step from 0 mV to -120 mV for 1 second during the application of 100 μ M MTSEA. The voltage steps occurred every 2 seconds. (D) Currents measured at the arrow in (B) as a function of cumulative exposure to MTSEA. Modification rates for MTSEA at 0 mV (\bullet) and at -120 mV (\circ). (E-H) State-dependent accessibility of L254C. Currents before (E), during (F), and after (G) the application of 100 μ M intracellular MTSEA. In (E) and (G), the voltage steps occur in 10 mV increments from -40 mV to -150 mV. In (F), voltage was held at 0 mV and then stepped to -120 mV for the test pulse, followed by a step to +50 mV for tail currents. The holding potential was -120 mV. The patch was

excised into a bath solution containing 100 μ M MTSEA. **(H)** Currents measured at the arrow in **(F)** as a function of cumulative exposure to MTSEA. Modification time course for intracellular MTSEA at 0 mV (**●**) and -120 mV (**□**). The current amplitudes are plotted versus cumulative exposure to MTSEA and MTSET, in **(D)** and **(H)**, respectively. The bold line is an exponential fit to the data in **(H)**.

b. The range of movement for S4

We next tested the accessibility of residues in proximity to 253 and 254 for the state-dependence of MTSET modification. We attempted to test the accessibility of residue R259C; however, this mutation did not express. Subsequent mutations on the adjacent residues L258C and L260C failed to express as well. S261C did express, and so this residue was used to test for internal accessibility (Fig. 5A-D). We found that the intracellular application of 200 μ M MTSEA modified S261C faster at -140 mV than at 0 mV (Fig. 5D, Table 1). This result suggests that S261C is more accessible from the intracellular side at hyperpolarizing potentials than at depolarizing potentials.

The mutant K250C, the next charged residue in the direction of the N-terminal, did not express, so we used I251C – an adjacent, uncharged residue. The extracellular application of MTSET to I251C did not affect currents either at 0 mV or -100 mV (Table 1). Intracellular accessibility studies were attempted on I251C, to test the range in intracellular S4 movement, but poor expression in patches prevented analysis. Thus, it remains unknown whether accessibility of I251C is state-dependent.

The extracellular application of MTSET onto R247C mutants dramatically decreased the deactivation times of tail currents (Fig. 5E-G). There was only a small difference in the MTSET modification rates between hyperpolarizing and

depolarizing potentials (Fig. 5H, Table 1), indicating that R247C is exposed to the extracellular solution both at depolarizing and hyperpolarizing potentials. The results for R247C are similar to the results for R332C, the homologous residue in spHCN channels [70].

The extracellular application of MTSET onto T249C mutants resulted in a shift in voltage activation to more hyperpolarizing potentials by about 10 mV. This modification was state-dependent, with modification rates faster at 0 mV than –100 mV (Fig. 5I-L, Table 1; see also Discussion). The voltage-dependent modification rates suggest that T249C moves from an extracellularly accessible location at depolarizing potentials to an inaccessible position at hyperpolarizing potentials. R247C and T249C did not express well enough to test for intracellular accessibility.

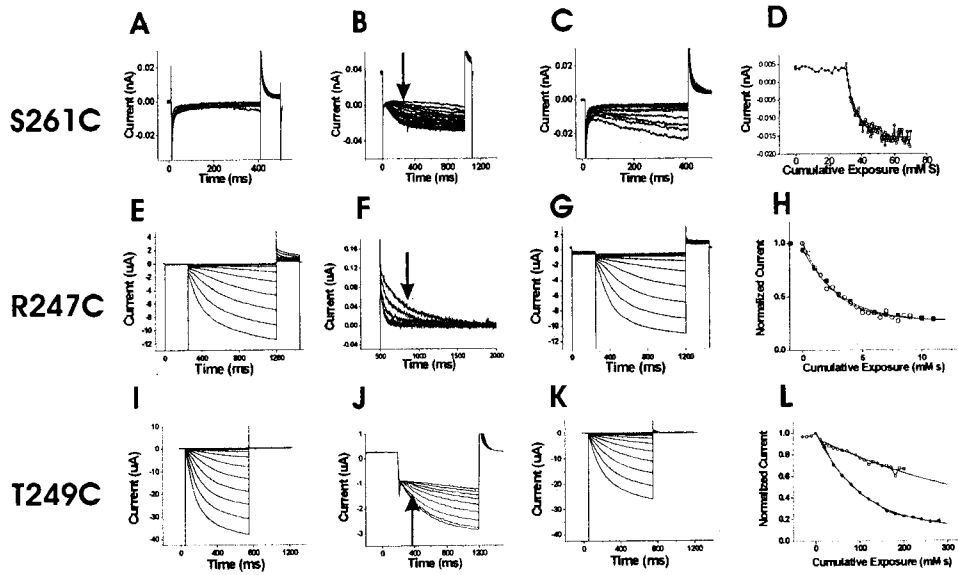


Figure 5. State-dependent accessibility of three S4 residues. (A-D) State-dependent accessibility of S261C. Currents before **(A)**, during **(B)**, and after **(C)** the intracellular application of 200 μ M MTSEA. In **(A)** and **(C)**, the voltage steps occur in -10 mV increments from -60 mV to -150 mV. In **(B)**, the voltage was held at 0 mV and then stepped to -140 mV for the test pulse, followed by a step to $+50$ mV for tail currents. The holding potential was 0 mV. The patch was excised into a bath containing 200 μ M MTSEA. **(D)** Modification time course for intracellular MTSEA at 0 mV (\bullet) and -140 mV (\square). The current amplitudes are plotted versus their cumulative exposure to MTSEA. The bold line is an exponential fit. **(E-G)** State-independent accessibility of R247C. Currents before **(E)**, during **(F)**, and after **(G)** the extracellular application of 100 μ M MTSET. In **(E)** and **(G)**, the voltage steps occur in -10 mV increments from 0 mV to -150 mV. In **(F)**, voltage was held at 0 mV and then stepped to $-$

120 mV for the test pulse, followed by a step to 0 mV for tail currents. The tail currents during the application of 100 μ M MTSET are shown in (F). (H) Currents at the arrow in (F) as a function of cumulative exposure to MTSET. The modification time course for the extracellular application of MTSET at 0 mV (\bullet) and at -100 mV (\square). The bold lines are exponential fits to the data. (I-L) State-dependent accessibility of T249C. Currents before (I), during (J), and after (K) the application of 2 mM extracellular MTSET. In (I) and (K), the voltage steps occur in -10 mV increments from 0 mV to -150 mV. In (J), voltage was held at 0 mV and then stepped to -120 mV for the test pulse, followed by a step to + 50 mV for tail currents. The holding potential was 0 mV. MTSET was applied for 10 seconds during each episode. (L) Currents at the arrow in (J) as a function of cumulative exposure to MTSET. Modification time course for the extracellular application of MTSET at 0 mV (\bullet) and at -100 mV (\square).

c. The COOH terminus and gating differences between HCN1 and spHCN

The state-dependent pattern of cysteine accessibility is very similar between spHCN [70] and HCN1 channels (this study), suggesting that S4 has a similar role in these two channels and that S4 is the voltage sensor in both these channels. However, the gating behavior of spHCN channels is quite different from the gating behavior in HCN1 channels: HCN1 channels do not inactivate, while spHCN channels display an inactivation that can be removed by a high concentration of cAMP (Fig. 6A&B). spHCN channels also activate at more depolarized potentials than mammalian HCN channels [16, 18].

The cAMP-binding site has been in the C-terminus that contains a consensus cyclic nucleotide-binding domain (CNBD). Earlier studies have shown that deleting the C-terminus (including the CNBD) from mammalian HCN channels eliminates the cAMP-induced voltage shifts [42]. To elucidate the role of the C-terminus in the different gating behavior between spHCN channels and HCN1 channels, we constructed a C-terminal-deleted spHCN channel spHCN_{ΔC-term} (see Methods). spHCN_{ΔC-term} channels did not inactivate in 0 cAMP solutions, in contrast to wt spHCN channels (n=3, Fig. 6C). In addition, the amplitude of the current through spHCN_{ΔC-term} channels did not change with cAMP concentration, in contrast to wt spHCN channels (n=3, Fig. 6D). The absence of inactivation in spHCN_{ΔC-term} channels shows that the inactivation of spHCN channels is not an intrinsic property of the transmembrane-containing portion (S1-S6) of spHCN channels, but requires the presence of the C-terminus. In

addition, the spHCN $_{\Delta C\text{-term}}$ channels activated at more hyperpolarized potentials ($V_{1/2} = -73 \pm 6$ mV and $z = 3.3 \pm 0.9$, $n=3$) than the wt spHCN channels ($V_{1/2} = -47 \pm 3$ mV and $z = 3.2 \pm 0.5$, $n=3$). The C-terminus-truncated versions of spHCN and HCN1 channels activated in a similar voltage range (Fig. 2C), suggesting that the C-terminus of spHCN channels is, at least partly, responsible for the more depolarized voltage range of activation of spHCN channels.

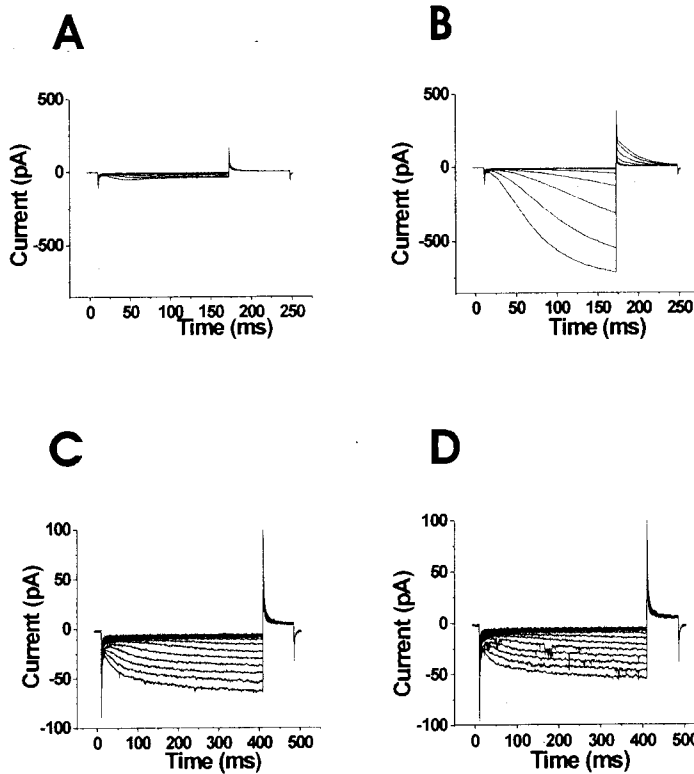


Figure 6. The C-terminus is necessary for inactivation in spHCN channels. Currents in the absence of internal cAMP (A, C) or the presence of 100 μ M cAMP (B, D) in inside-out patches expressing wt spHCN channels (A, B) and spHCN Δ C-term channels (C, D). For the wt spHCN channels, voltage steps occurred in 10 mV increments from -10 mV to -120 mV, from a holding potential of -10 mV. Tail currents were at $+50$ mV. For the spHCN Δ C-term channels, voltage steps occurred in 10 mV increments from -10 mV to -160 mV, from a holding potential of -10 mV. Tail currents were at $+50$ mV. The effects of the truncation of the C-terminus of spHCN channels are: 1) the removal of inactivation, 2) a shift in the voltage dependence by -25 mV (see

text), and 3) a 10-fold reduction in the expression level. (Note that spHCN channels in the excised patches activated at 20-30 mV more negative potentials than in intact oocytes, [70]).

E. Discussion

Using cysteine accessibility methods, we found that S4 moves in a voltage-dependent manner in HCN1 channels (Table 1 and Fig. 7C). The opposite state-dependent accessibility of two neighboring residues, S253C and L254C, suggests that the middle portion of S4 moves completely across the membrane when the HCN1 channel goes from the closed state to the open state (Fig. 7A&B). This S4 movement is similar to the S4 movement previously found in spHCN channels [70] and in Shaker K⁺ channels [55, 72], in which residues S338 in spHCN and R368 in Shaker K⁺ channels (homologous to S253 in the HCN1 channel) exhibited a voltage-dependent transmembrane movement from the intracellular solution to the extracellular solution. Data from other cysteine mutations, such as S261C and T249C, provide additional support for a similar S4 motion in spHCN and HCN1 channels, and for a similar voltage-sensing mechanism in these channels (Fig. 7A & B). However, Bell and Siegelbaum (this issue) tested more intracellular residues and found that the intracellular S4 region that displayed state-dependent modification was significantly larger than the state-dependent extracellular S4 region. Therefore, we also suggest an alternative model for S4 movement in HCN channels (Fig. 7D & E), in which the S4 helix unwinds in the middle when S4 moves inward. This model is compatible with our data and provides an explanation for the smaller region of state-dependent modification at the external membrane border of S4 (Table 1; and see Bell and Siegelbaum, this issue).

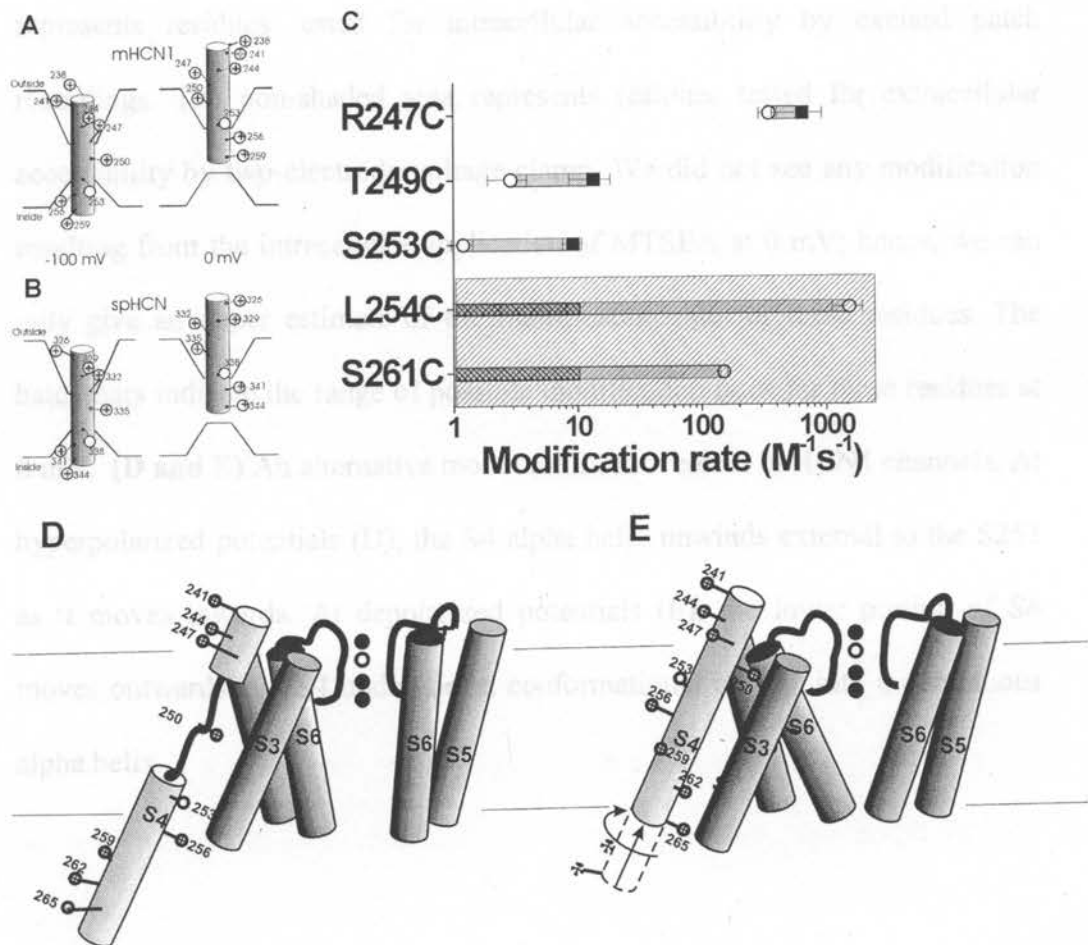


Figure 7. A model of the voltage-dependent movements of S4 in the HCN1 channel (A) and the spHCN channel (B). (A) Based on results from this study, S4 is the voltage sensor in the HCN1 channel. HCN1 S4 is in an inward position at -100 mV, which opens the channel gate. Stepping the voltage to 0 mV results in the outward movement of S4 into the extracellular solution, causing the channel gate to close. This movement is similar to that described for the spHCN channel [70], seen in (B). The intracellular border of S4 movement

is not well-defined from our results. **(C)** Modification rates for cysteine mutants in the HCN1 channel in the open (o) and closed (■) states. The shaded area represents residues tested for intracellular accessibility by excised patch recordings. The non-shaded area represents residues tested for extracellular accessibility by two-electrode voltage clamp. We did not see any modification resulting from the intracellular application of MTSEA at 0 mV; hence, we can only give an upper estimate of the modification rate for these residues. The hatch bars indicate the range of possible modification rates for these residues at 0 mV. **(D and E)** An alternative model for S4 movement in HCN1 channels. At hyperpolarized potentials (D), the S4 alpha helix unwinds external to the S253 as it moves inwards. At depolarized potentials (E), the lower portion of S4 moves outwards and S4 undergoes a conformational change into a continuous alpha helix.

In general, the state-dependence of intracellular modification was larger than that of extracellular modification (Fig. 7C). This finding could be due to the limited voltage range for testing MTSET accessibility in intact oocytes (-100 mV to +50 mV), in combination with the fact that most of the cysteine-introduced HCN1 channels activated in a very hyperpolarized voltage range ($-120 \text{ mV} < V_{1/2} < -80 \text{ mV}$; Fig. 2C). We tested intracellular modification for closed channels at 0 mV, which is $>80 \text{ mV}$ from the mid-point of the activation curve. In most batches of oocytes, we were unable to test extracellular modification for open channels held at more negative potentials than -100 mV , a potential at which a significant number of channels remain closed, and, hence, a substantial number of S4s are most likely not in their activated position (Fig. 7A). The possibility that a substantial number of S4s are still in their resting position at -100 mV , could lead to an underestimation of the change in modification rate between closed and open channels. At a particular voltage, one could estimate the number of S4s in their resting versus activated position from the $G(V)$, but this estimation is very model-dependent. For example, S4 in HCN channels could move in several steps, and some of these steps could be concerted conformational changes in all four subunits, as has been suggested for Shaker K channels [72, 82-84]. If this were the case, then for a cysteine residue that becomes buried in a final concerted step, a fraction f of channels that are still closed would result in a fraction f of those cysteines to be accessible. On the other hand, a simple Hodgkin and Huxley model (4 independent S4s with only one resting position and one activated position) would, at the same open

probability, predict that a much smaller fraction of these cysteines would be accessible (see Bell and Siegelbaum, in this issue). A gating charge versus voltage curve would give a better estimate of how many S4s are in the resting position relative the activated position at any potential. To this day, there are no published recordings of gating currents from HCN1 channels. However, we were able to measure the external accessibility of 249C at -130 mV in one batch of oocytes (Fig. 8). The modification rate at -130 mV was >40 fold slower at -130 mV than at 0 mV, measured in the same oocyte ($k < 0.33 \text{ M}^{-1}\text{s}^{-1}$ at -130 mV; $k = 13.5 \text{ M}^{-1}\text{s}^{-1}$ at 0 mV, $n = 4$). From the limiting data on extracellular accessibility at extremely negative voltages, we have concluded that the accessibility of S4 changes with voltage both at the extracellular and the intracellular membrane border. Hence, we conclude that S4 movement is similar in HCN1 channels and spHCN channels.

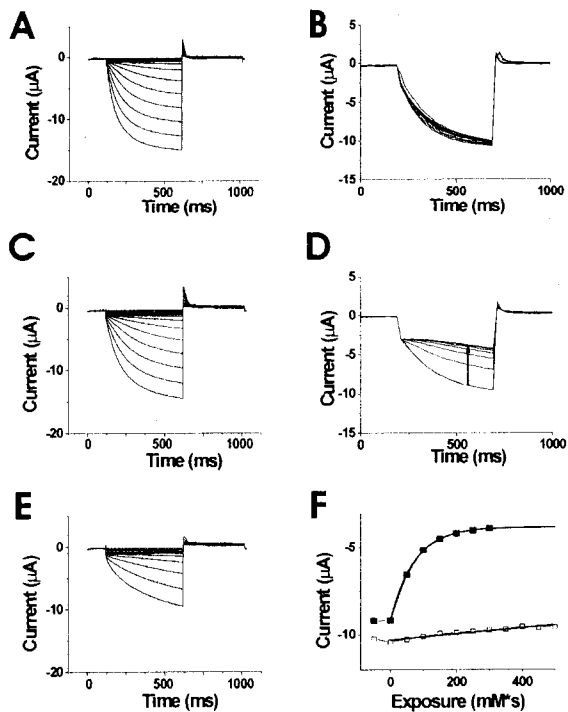


Figure 8. Larger state-dependent modification of T249C at more hyperpolarized potentials. Currents before (A), during (B), and after (C) the application of 10 mM extracellular MTSET applied at -130 mV. Currents during (D) and after (E) the application of 10 mM extracellular MTSET applied at 0 mV on the same oocyte as in (A) to (C). In (A), (C), and (E), the voltage steps are in -10 mV increments from 0 mV to -140 mV. In (B) and (D), the voltage was held at 0 mV and then stepped to -120 mV for the test pulse, followed by a step to $+50$ mV for tail currents. The holding potential was 0 mV.

MTSET was applied for 5 seconds between each episode. **(F)** Currents measured at the arrow in **(D)** as a function of cumulative exposure to MTSET. The modification time course for extracellular application of MTSET at 0 mV (**■**) and at -130 mV (**□**). The bold lines are an exponential fit to the data (for -130 mV, the I_{∞} was constrained to the value found for the fit at 0 mV). $\tau = 3.5$ M*s for -130 mV, and $\tau = 0.0727$ M*s for 0 mV. Similar results were seen in 4 oocytes.

However, there are significant functional differences between spHCN channels and mammalian HCN1 channels, in particular the presence of a cAMP-dependent inactivation in spHCN [18], which is absent in mammalian HCN channels. In addition, spHCN channels open in a more depolarized voltage range [16, 18]. We found that the deletion of the C-terminus in spHCN channels removed the inactivation of spHCN channels, showing that the inactivation of spHCN channels is not an intrinsic property of the transmembrane-containing portion (S1-S6) of spHCN. This inactivation can also be removed by high concentrations of cAMP that presumably bind to the CNBD domain in the C-terminus. The removal of inactivation by either high concentrations of cAMP or by a C-terminal-deletion mutation lead us to suggest a model for the inactivation of spHCN channels that is similar to a model proposed to explain the cAMP-dependent voltage shifts in the mammalian HCN channels [42]. In the model proposed by Wainger et al. (2001), in the absence of cAMP the C-terminus inhibits the transmembrane-containing portion of the HCN channel, causing a hyperpolarizing shift in the voltage dependence. The binding of cAMP to the C-terminus or the deletion of the C-terminus relieves this inhibition, resulting in the shift of the voltage dependence to more depolarized potentials [42]. We propose that in spHCN channels, at low cAMP the C-terminus interacts with the transmembrane-containing portion (S1-S6) of spHCN, causing the inactivation of spHCN channels and a reduction in current amplitude. High concentrations of cAMP or a deletion of the C-terminus removes this interaction, thus relieving the inactivation.

The deletion of the C-terminus also shifted the voltage dependence of spHCN channels by -25 mV, making the truncated spHCN channels open in a voltage range similar to the voltage range in the mammalian HCN channels. In contrast, the truncation of HCN1 channels shifted the activation range of HCN1 channels only by a very small amount in the opposite direction (+5 mV; [42]), suggesting that the more depolarized activation range of spHCN channels could be due to the stabilization of the open state relative the closed state by the C-terminus. This effect is opposite to the one seen in mammalian HCN channels, where the C-terminus stabilizes the closed state [42]. In addition, this effect in spHCN channels is not modulated by cAMP, whereas the effect in mammalian HCN channels is cAMP dependent [42]. One attractive mechanism for the effect seen in spHCN channels is an electrostatic interaction between some of the positive charges in S4 and some negative charges in the C-terminus of spHCN channels. This interaction would stabilize the inward position of S4 and, hence, would shift the voltage dependence to more depolarized potentials. The C-terminus in spHCN channels contains additional negative charges that are not present in the mammalian HCN channels. In the crystal structure of the C-terminal domain of HCN2 channels [44], several of these additional negative charges are located on the surface of this structure, where they could possibly interact with other domains of the channel (e.g., with positive charges in S4). Another possibility is that the C-terminus in spHCN channels destabilizes the closed state by directly affecting S6, which has been suggested to be the activation gate of HCN

channels [32, 40]. This hypothesis is supported by the activation kinetics slowing in the C-terminus-deleted spHCN channels at extreme negative potentials (Fig. 6). Further studies are necessary to elucidate the mechanism of C-terminus modulation of spHCN channels and to determine whether the difference between spHCN and mammalian HCN channels is caused by a difference in the C-terminus or a difference in the interaction between the C-terminus and the core domain. However, it is clear that the C-terminus of spHCN channels has two effects on spHCN channels: a cAMP-dependent effect that causes inactivation and a cAMP-independent effect that shifts the voltage dependence into a more depolarized voltage range.

Our cysteine accessibility results suggest that the four most N-terminal S4 charges in HCN1 channels (K238, R241, R244, and R247) and the three most N-terminal S4 charges in spHCN channels (R326, K329, and R332) [70] are not part of the voltage sensor. The state-independent accessibility of R247 in HCN1 channels, and R326C and R332C in spHCN channels [70] indicate that these charges are always exposed to the extracellular solution and, hence, do not significantly contribute to the voltage sensor since they do not traverse a significant part of the electric field. However, the neutralization of these charges changes the voltage dependence by shifting the activation curve to more negative potentials in both spHCN channels and mammalian HCN channels [59, 60, 70] showed that altering the charge on the corresponding residues in HCN2 channels alters the size of Mg^{2+} -induced voltage shifts in a manner consistent

with these residues functioning as surface charges. Our results, showing that these residues are always exposed to the extracellular solution, support the hypothesis by Chen et al. (2000) that these charges function as surface charges. Alternatively, these most external charges might serve to stabilize the closed state or destabilize the open state by interacting with other charged parts of the channel. The neutralization of these charges could, therefore, shift the equilibrium between the open and closed states, giving rise to the observed voltage shifts. In both cases, these external residues only indirectly influence the voltage sensitivity of HCN channels since they do not directly form part of the voltage sensor of HCN channels.

These external charges are conserved among HCN channels. Why are these charges conserved if they are not part of the voltage sensor? Our results are consistent with the hypothesis that these charges function as surface charges. We hypothesize that these surface charges are necessary for the HCN channels to open in a physiologically relevant voltage range. This hypothesis is based on the finding that the removal of these charges in mammalian HCN channels shifts the voltage dependence to such negative potentials that, under normal physiological conditions ($V > -80$ mV), these channels seldom open [59, 60].

Hyperpolarization-activated HCN channels appear to share a similar S4 movement with depolarization-activated Kv channels. However, in HCN channels, the outward movement of S4 is related to channel closing, and the

inward movement of S4, to channel opening. These S4 movements are the opposite from those in Shaker K⁺ channels, where the outward movement of S4 leads to channel opening and the inward movement leads to channel closing. The coupling mechanism between the movement of the voltage sensor and the opening of the activation gate remains undefined for both HCN channels and Kv channels [85]. A more detailed analysis of the movement of S4 and the identification of the molecular interactions between S4 and the pore region S5-S6 in HCN and Kv channels may give more insight into the coupling mechanisms of these two classes of channels and could help explain the structural basis for the opposite voltage dependence of activation that exists between hyperpolarization- and depolarization-activated channels.

III. Chapter 3

Intracellular Mg^{2+} is a voltage dependent pore blocker of HCN channels

Sriharsha Vemana, Shilpi Pandey, and H. Peter Larsson

Neurological Sciences Institute
Oregon Health & Science University
505 NW 185th Avenue
Beaverton OR 97006

Correspondence to H. Peter Larsson, Neurological Sciences Institute, Oregon Health & Science University, 505 NW 185th Avenue, Beaverton, OR 97006. E-mail: larssonp@ohsu.edu, Phone: 503-418-2655, Fax: 503-418-2501

Condensed title: Vemana et al., Magnesium blocks outward HCN currents

Acknowledgements.

We thank Drs. Andrew Bruening-Wright and Fredrik Elinder for comments and suggestions on the manuscript. This work was supported by NIH grant NS043259.

A. Abstract

Hyperpolarization-activated cyclic nucleotide-gated (HCN) channels are activated by membrane hyperpolarization that creates time-dependent, inward-rectifying currents, gated by the movement of the intrinsic voltage sensor S4. However, inward rectification of the HCN currents is not only observed in the time-dependent HCN currents, but also in the instantaneous HCN tail currents. Inward rectification can also be seen in mutant HCN channels that have mainly time-independent currents [66]. In the following paper, we show that intracellular Mg^{2+} functions as a voltage-dependent blocker of HCN channels, acting to reduce the instantaneous outward currents. The affinity of HCN channels for Mg^{2+} is in the physiological range, with Mg^{2+} binding with an IC_{50} of 0.53 mM at +50 mV in HCN2 channels. The effective electrical distance for the Mg^{2+} binding site was found to be 0.19. Removing a cysteine in the selectivity filter reduced the affinity for Mg^{2+} suggesting that this residue forms part of the binding site deep within the pore. Our results show that Mg^{2+} acts a voltage-dependent pore blocker and, therefore, reduces outwards currents through HCN channels. The pore blocking action of Mg^{2+} may play an important physiological role, especially for the slowly gating HCN2 and HCN4 channels. Mg^{2+} could potentially block outward hyperpolarizing HCN currents at the plateau of action potentials, thus preventing a premature termination of the action potential.

B. Introduction

Rhythmic activity of “pacemaker” cells in the heart and thalamic neurons in the brain are dependent on the inward I_h current through hyperpolarization-activated cyclic-nucleotide-gated (HCN) channels [15, 25]. Following an action potential in pacemaker cells, I_h contributes to the currents that slowly depolarize the membrane potential to threshold, thereby initiating another action potential [5]. Four mammalian HCN channels have been cloned: HCN1-HCN4 [16, 18, 86]. The deletion of HCN channels, or the presence of naturally occurring mutations in HCN channels, has been shown to have significant physiological consequences [30, 87-89]. HCN2 knockout mice, for example, showed spontaneous absence seizures and cardiac sinus dysrhythmia [30].

HCN channels are members of the super family of voltage-gated ion channels, possessing features such as a tetrameric structure, with each subunit containing six transmembrane domains (S1-S6) [15, 25]. In addition, HCN channels have a pore domain that shows conservation with voltage-gated potassium (Kv) channels, including a GYG signature motif in the selectivity filter, even though HCN channels are only modestly more selective for K^+ over Na^+ (3:1) [16, 18]. Similar to Kv channels, HCN channels have an intracellular gate at the base of S6 that prevents access of ions to the pore [40, 90]. Both Kv and HCN channels have a positively charged S4 domain that acts as the voltage sensor, controlling the opening and closing of the gate in response to membrane voltage [70, 71, 91, 92]. Despite the conservation of S4 movement between HCN and Kv

channels, the outward S4 movement in response to depolarization has opposite effects in the two types of channels. Depolarization opens the gate of Kv channels, but closed the gate of HCN channels [70, 85]. This inverse S4-to-the-gate coupling, when compared to Kv channels, and the relative non-selective cation permeability of HCN channels allow HCN channels to mediate a hyperpolarization-activated, depolarizing inward current that contributes to a variety of physiological functions in the body [25, 93].

The hyperpolarization-activation of HCN channels conferred by the S4 movement generates time-dependent, inward-rectifying currents through HCN channels. However, during two-electrode recordings of HCN channels (Bruening-Wright et al. in press), we noticed that the instantaneous currents in these channels were also inwardly rectifying. For example, in response to voltage protocols designed to measure the instantaneous tail currents at different voltages following an activation prepulse to -120 mV, the inward instantaneous currents were at least twice as large as the outward instantaneous currents for similarly sized, but opposite, driving forces. In addition, mutations in the S4-S5 loop and S6 that removed the time-dependence of the HCN currents, presumably by locking HCN channels in the open state, still displayed time-independent, inward-rectifying currents [66]. Using excised patches containing HCN channels, we tested whether an intracellular blocking agent is responsible for this rectification or whether this rectification is due to an intrinsic voltage-gating property of HCN channels. Based on the following data, we suggest that

intracellular magnesium binds in the pore of HCN channels in a voltage dependent manner, thereby generating inwardly rectifying instantaneous HCN currents.

C. Methods

a. Molecular Biology

The mouse HCN1 and HCN2 channels were used in this study. The HCN1 channels had the C-terminal deleted and a small region in the N-terminal deleted that maximize the expression in oocytes [42]. The HCN2 channel had GC rich domains in the N- and C-terminus deleted to facilitate the use of molecular biology techniques on the HCN2 DNA [66]. Site-directed mutagenesis was performed on HCN1 channels to create mutations C347S, C347G, and C347A using the QuickChange Kit (Stratagene). The mutation C347T in HCN1 was a generous gift from Dr. Steven Siegelbaum (Columbia University). The mutation R318Q/Y331S in HCN2 was a generous gift from Dr. Michael Sanguinetti (University of Utah). The HCN1 DNA was linearized with Nhe1 and the HCN2 DNA was linearized with EcoR1. RNA was synthesized in vitro using the T7 mMessage mMachine kit (Biocrest). RNA was injected (50 nl of 0.1-1 ng/nl) into *Xenopus* oocytes, and experiments were performed 2 to 7 days after injection.

b. Electrophysiology

The macro-patch currents were measured with the patch-clamp technique using an Axopatch 200B amplifier (Axon Instruments, Inc.). The pipette solution consisted of a 100-K solution (in mM): 100 KCl, 1.5 MgCl₂, 10 HEPES. In

addition, 1 mM BaCl₂, 100 μM LaCl₃, and 100 μM Gadolinium were added to the pipette solution to block endogenous currents including voltage-dependent potassium currents, hyperpolarization-activated chloride currents, and calcium-activated chloride currents. The patch pipettes had a resistance of around 1 MΩ. The bath solution consisted of a 100-K solution (in mM): 98 KCl, 5 NaCl 1 EGTA, 10 HEPES, 1 EDTA and 100 μM cAMP. A separate solution without EDTA was used for the intracellular application of MgCl₂. This solution consisted of (in mM): 98 KCl, 5 NaCl, 1 EGTA, 10 HEPES. To this solution, we added ascending concentrations of MgCl₂, including, 0.25 mM, 0.5 mM, 1 mM, 5 mM, 10 mM, and 20 mM. 100 μM cAMP was also added to saturate the cAMP binding site in the HCN channels. An EVH-9 perfusion system (BioLogic Science Instruments) was used to rapidly alternate between the different MgCl₂ concentrations applied to the cytosolic side of excised patches.

D. Results

a. Instantaneous rectification is not due to an intrinsic voltage-dependent process

Figure 9 shows the currents from HCN1 channels recorded in the cell-attached mode from *Xenopus* oocytes in symmetrical 100 mM K solutions (assuming 100 mM K in the cytosol of the oocytes). The HCN currents exhibit the characteristic hyperpolarization-activated, time-dependent currents caused by HCN channel opening in response to negative voltage steps and the time-dependent closing in response to a depolarizing voltage step (Fig. 9A). A closer inspection of the currents, however, revealed that the amplitude of the outward currents was smaller than expected. The outward tail currents at +50 mV were not proportional to the inward currents, when normalized to the driving force at the different voltage steps (Figs. 9A). These, smaller than expected, tail currents suggest that there is some inward rectification of the instantaneous currents in HCN channels. To further visualize the inward rectification, we stepped to a negative potential (-140 mV) to open all HCN channels, followed by voltage steps to various potentials to record both outward and inward instantaneous currents (Figs. 9B). Inward rectification is clearly evident in the plots of the instantaneous HCN1 current amplitude against voltage (Figs. 9C). HCN2 channels exhibited a similar inward rectification in the instantaneous currents (data not shown).

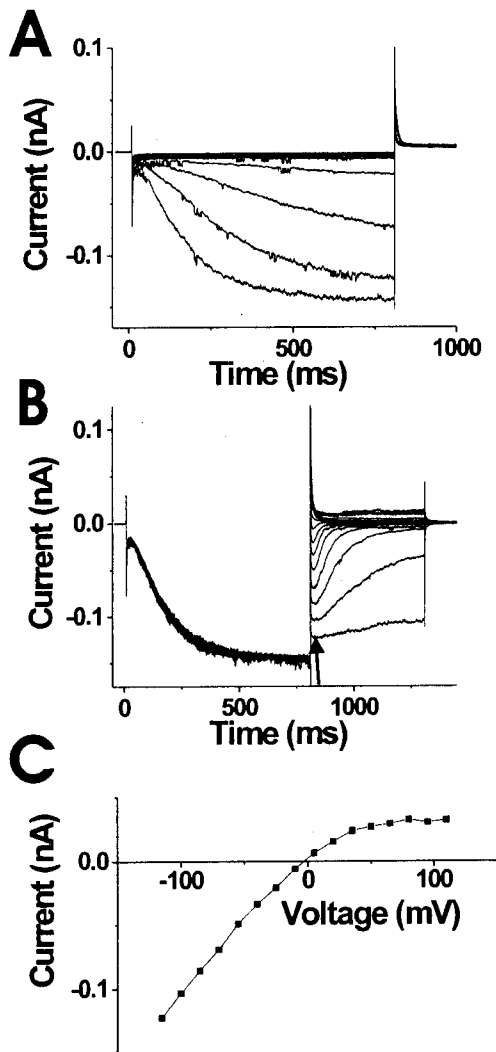


Figure 9. HCN channels show rectification in cell-attached patches.

(A) HCN1 currents elicited by voltage steps from -30 mV to -150 mV (in -10 mV increments), from a holding potential of 0 mV, followed by a step to +50 for tail currents. (B) HCN1 tail currents elicited by voltage steps from +110 mV to -115 mV (-15 mV increments), following a prepulse to -130 mV. Holding potential =

0 mV. (C) Current versus voltage (I/V) plot measured at the arrow in B. Inward rectification is clearly seen in the instantaneous currents.

To test whether this inward rectification is due to an intracellular factor in the oocytes, we measured HCN1 and HCN2 currents in cell-free, excised patches. Upon excision of HCN1 and HCN2 patches into a 100 K internal solution (100K, 10 HEPES, 1 EGTA, 1 EDTA, pH=7.2), the size of the tail currents increased approximately two-fold: $122\% \pm 24$ ($n = 5$) (Figs. 10A and 10B) in HCN1 channels and $55\% \pm 21$ ($n = 3$) in HCN2 channels (Figs. 10C and 10D). The instantaneous currents in excised patches had a linear I/V in this intracellular solution and lacked the inward rectification found in cell-attached patches (Figs. 10E and 10F), suggesting that an intracellular agent is responsible for the inward rectification in intact oocytes. To further test whether an intracellular agent within the oocyte was responsible for the observed changes in tail amplitudes upon excision, we returned the excised patch back into the intracellular environment within the oocyte by using patch cramming (i.e. forcing the patch into the oocyte cytosol thereby exposing the intracellular side of the membrane again to the oocyte cytosol) [94]. Upon patch cramming, the outward tail currents returned immediately to their smaller size and the instantaneous currents once again became inwardly rectifying (Fig. 11). The linear instantaneous I/V in excised patches suggests that it is not an intrinsic voltage-dependent process in HCN channels that causes the inward rectification in the instantaneous currents, but that an intracellular agent is responsible for the reduction in amplitude of the outward currents.

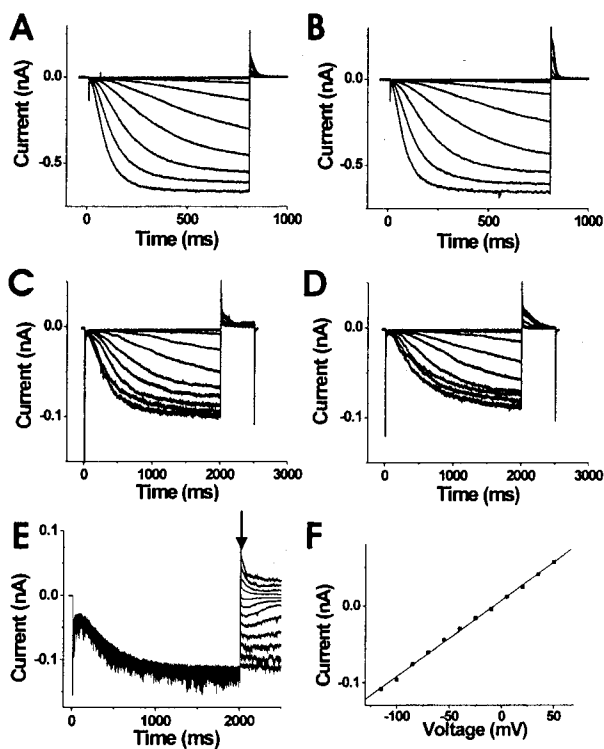


Figure 10. HCN1 and HCN2 tail currents increase in amplitude after excision. (A-B) HCN1 currents in cell attached (A) and excised (B) patches elicited by voltage steps from -30 mV to -150 mV (in -10mV increments), followed by a step to +50 for tail currents. Holding potential = 0 mV. (C-D) HCN2 currents in cell attached (C) and excised (D) patches elicited by the same protocol as in A. (E) HCN2 currents in an excised patch in response to a -120 mV activation prepulse followed by voltage steps from +50 mV to -115 mV (in -15 mV increments). (F) Plot of current versus voltage for HCN2 tail currents (measured at the arrow in E) after patch excision. The I/V was fitted with a straight line.

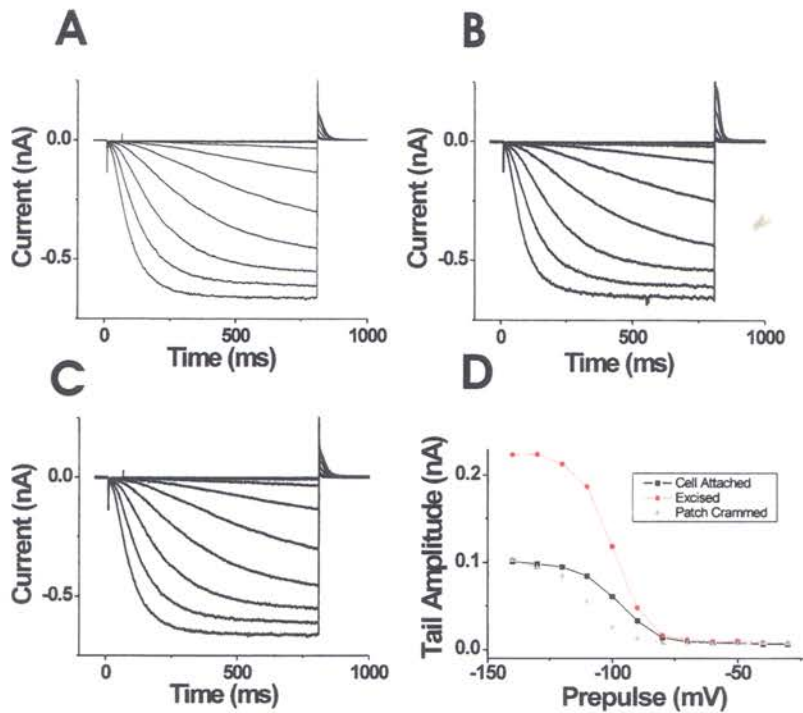


Figure 11. Patch cramming reduces the amplitude of the outward currents back to cell attached levels. (A-C) Currents from an HCN2 channel elicited by voltage steps from -30 mV to -150 mV (in -10mV increments), followed by a step to +50 for tail currents. Holding potential = 0 mV. (A) Cell attached patch, (B) excised patch, and (C) patch crammed into the cytoplasmic environment of the *Xenopus* oocyte. (D) A plot of tail current amplitude versus the prepulse voltage (D) in a cell attached patch (■), an excised patch (●), and a patch inserted back into the *Xenopus* oocyte (▲). The approximately -10mV shift seen between the cell-attached patch and the patch reinserted back into the *Xenopus* oocyte is most likely due to degradation of some of the membrane-bound PIP₂, which has been shown to shift the voltage dependence of HCN channels by >20 mV [95]

b. Intracellular Mg^{2+} blocks HCN currents at physiological

concentrations

We next tested different cytosolic agents that could potentially cause the inward rectification of the instantaneous currents in HCN channels. In inward-rectifying K^+ channels, it has been shown that the inward rectification is mainly due to a voltage-dependent block by intracellular Mg^{2+} and polyamines, such as spermidine and spermine [96, 97]. The *Xenopus* oocyte cytosol contains approximate 1 mM free Mg^{2+} and 10 μ M of free polyamines, such as spermidine and spermine [98, 99]. We therefore tested the effect of applying physiological concentrations of Mg^{2+} , spermidine, and spermine to the cytosolic side of excised patches, in order to determine whether Mg^{2+} and polyamines block the outward currents through HCN channels (Fig. 12). Both the application of 10 μ M spermine and the application of 10 μ M spermidine blocked the outward currents through HCN1 channels. 10 μ M spermine blocked the currents at +50 mV by $9\% \pm 3.6$ ($n = 3$) and 10 μ M spermidine blocked the currents at +50 mV by $16.3\% \pm 4.0$ ($n = 3$). However, the amount of block of the outward HCN currents induced by these polyamines was less than the block seen in intact oocytes (Figs. 12B and 12C). In contrast, the application of 1 mM Mg^{2+} blocked the currents at +50 mV by $38.3\% \pm 7.2$ ($n = 3$) in HCN1 channels (Figs. 12B and 12C). That physiological concentrations of Mg^{2+} had the most potent block of the instantaneous currents suggests that it is mainly Mg^{2+} that causes the inward rectification of instantaneous HCN currents in intact cells.

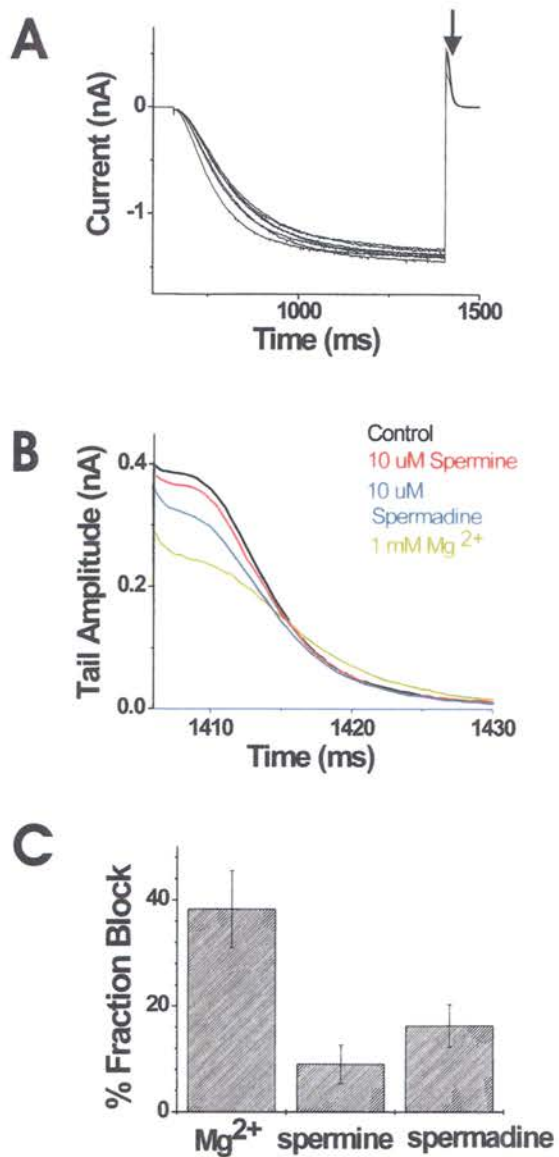


Figure 12. Physiological concentrations of intracellular magnesium block HCN outward current more than spermine or spermadine. (A) HCN currents elicited by a -130 mV step from a holding potential of 0 mV, followed by a step to +50 mV for tail currents, during perfusion of control solutions, 10 μ M Spermidine, 10 μ M Spermine, and 1 mM Mg^{2+} . (B) Enlargement of the tail

currents showing the four sweeps where control solution (black), 10 μM Spermidine (green), 10 μM Spermine (blue), and 1 mM Mg^{2+} (red) were applied. Between every trace where a potential blocker was applied, an application of 100-K control solution was applied (not shown). (C) A quantitative summary of the % fraction of tail current blocked for Mg^{2+} , spermine and spermidine.

c. Mg^{2+} blocks HCN currents in a voltage dependent manner

We next measured the affinity of Mg^{2+} for HCN1 and HCN2 channels by applying different concentrations of Mg^{2+} and measuring the size of the outward tail currents at +50 mV, following an activation prepulse to -130 mV to open all channels. The tail currents decreased for increasing Mg^{2+} concentrations including (in mM) 0.25, 0.5, 1, 5, 10 and 20 (Figs. 13A and 13B). The dose response curve was well fit with a Michaelis-Menton curve with a Hill coefficient of 1.11 ± 0.04 ($n = 3$). The IC_{50} was $0.82 \text{ mM} \pm 0.27 \text{ mM}$ at +50 mV ($n = 3$) for HCN1 channels (Fig. 13C) and the IC_{50} was $0.53 \text{ mM} \pm 0.12 \text{ mM}$ ($n = 3$) at +50 mV for HCN2 channels (Fig. 13D). The higher concentrations of Mg^{2+} also changed the kinetics of the currents (Fig 13A). Higher concentrations of Mg^{2+} slowed the opening of the channels. The voltage dependence of opening was also shifted to more hyperpolarized potentials with higher concentrations of Mg^{2+} (data not shown). Mg^{2+} probably caused these effects by screening surface charges close to the voltage sensor. These effects were not further studied here.

The rectification induced by intracellular Mg^{2+} (Fig. 9) suggests that Mg^{2+} binding is voltage dependent. The voltage dependence of Mg^{2+} block was determined by measuring the IC_{50} at different tail potentials for HCN1 channels (Fig. 14). The affinity for Mg^{2+} was clearly voltage dependent: the IC_{50} was $0.81 \text{ mM} \pm 0.23$ ($n = 3$) at +80 mV and $1.8 \text{ mM} \pm 0.1$ ($n = 3$) at +20 mV (Fig. 6A). The Mg^{2+} affinity versus voltage was fit to the Woodhull equation [100], $Mg^{2+}(V) = Mg^{2+}(0 \text{ mV}) / (1 + \exp(-\delta * z * V / kT))$. The electrical distance (δ) was

found to be 0.19 ± 0.06 ($n = 3$) and the Mg^{2+} affinity at 0 mV, $Mg^{2+}(0 \text{ mV})$, was found to be $2.3 \text{ mM} \pm 0.47$ ($n = 3$) (Fig. 14B). Mg^{2+} block of HCN2 channels displayed a similar voltage dependence (Fig. 14C). This shows that Mg^{2+} blocks HCN channels in a voltage dependent manner.

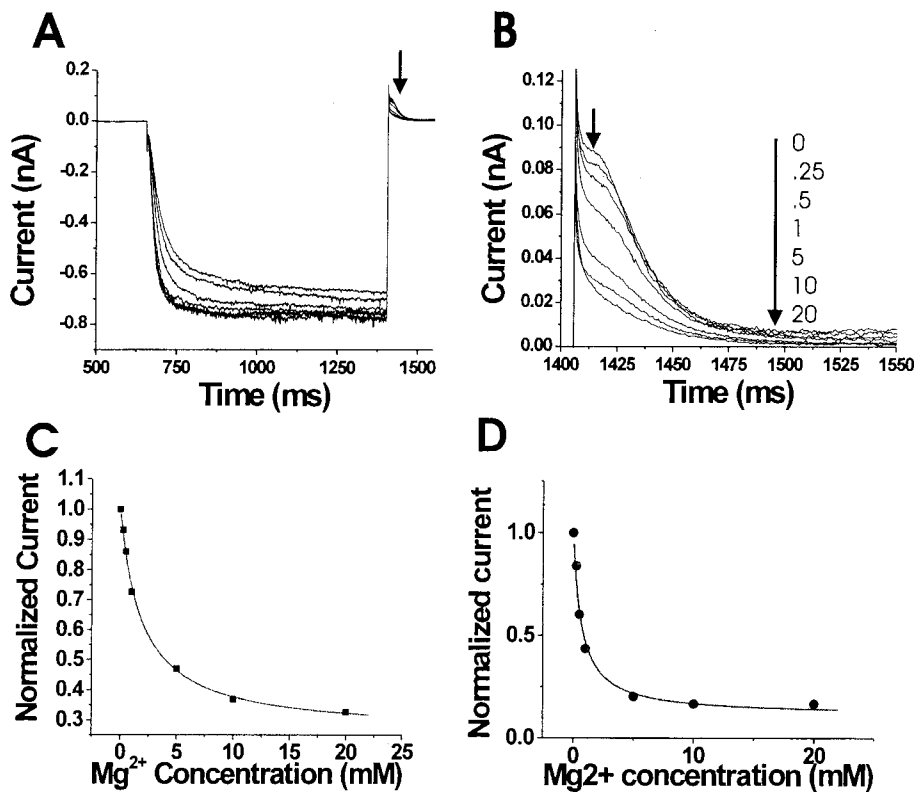


Figure 13. Mg²⁺ blocks HCN outward currents at physiological concentrations. (A) To test Mg²⁺ block of HCN1 outward currents, different concentrations of Mg²⁺ was applied while recording the currents in response to voltage step to -130 mV from a holding potential of 0 mV, followed by a voltage step to + 50 mV for tails. 0 Mg²⁺ was applied during the first sweep; followed in succession by different concentrations of Mg²⁺: (in mM) 0.25, 0.5, 1, 5, 10, and 20. (B) A close-up of the tail currents shows the concentration-dependent block of the outward tail currents in response to increasing concentrations of Mg²⁺. The arrow marks the time point at which values were

taken to create a dose-response curve for Mg^{2+} block of an HCN1 channel. (C) Dose-response curve for Mg^{2+} block of the currents through HCN1 channel at +50 mV. The values were fit with the equation: $I(Mg^{2+}) = I_{max}/(1 + K_m/[Mg^{2+}]) + C$. (D) Dose response curve for Mg^{2+} block of the currents through HCN2 channel at +50 mV, from similar experiment as in A.

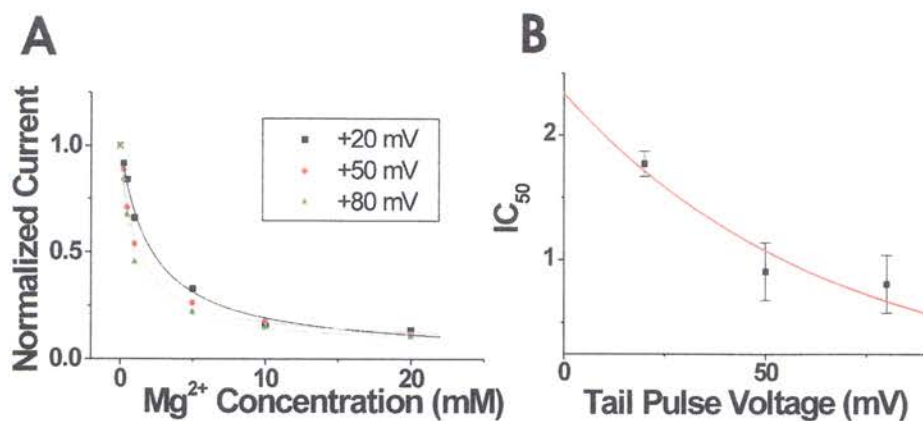


Figure 14. Voltage dependence of Mg^{2+} block. (A) Seven different concentrations of Mg^{2+} were applied while recording the currents from HCN1 channels in response to a voltage step to -130 mV, followed by a voltage step to either +20 mV, +50 mV or +80 mV. Holding potential = 0 mV. The order of application for Mg^{2+} was (in mM) 0, 0.25, 0.5, 1, 5, 10, 20. Current amplitudes from time points during the tail currents were used (as in Fig. 5) to create dose response curves for each of the three different tail voltages applied. (B) The IC_{50} values for the Mg^{2+} block of the tail currents at +20mV, +50mV, and +80mV plotted and fitted to the Woodhull equation: $Mg^{2+}(V) = Mg^{2+}(0 \text{ mV}) / (1 + \exp(-\delta \cdot z \cdot V / kT))$. The fraction of the membrane electric field traversed by the Mg^{2+} ion was $\delta = 0.19$. The intersection of the fitted line with the Y axis gave the K_m value at 0 mV: $Mg^{2+}(0 \text{ mV}) = 2.3 \text{ mM}$.

d. The effect of a pore mutation suggests that Mg^{2+} binds to the selectivity filter

The voltage dependence of Mg^{2+} block could be explained by Mg^{2+} blocking the outward currents by binding to a binding site in the pore of the HCN channels. Divalent ions have been shown to block currents in other channels by binding to sites in or near the selectivity filter in the pore. For example, in the KcsA channels, it has been shown by X-ray crystallography that Ba^{2+} binds to a binding site just below the GYG motif in the selectivity filter [101]. In HCN channels, Cd^{2+} has been shown to bind to a cysteine (C347 in HCN1) located two amino acids before the GYG [36]. In the KcsA crystal structure, the four homologous residues to this cysteine, one from each subunit, are very close together in space and could easily form an ion-binding site (Fig. 17). In contrast, the acidic residues in S6 that has been identified to bind Mg^{2+} in inward rectifying Kir channels [102, 103] is not conserved in HCN channels. We therefore tested whether mutations of C347 would affect Mg^{2+} binding to HCN channels.

The mutation C347S in the HCN1 channel was still susceptible to block by intracellular Mg^{2+} (Fig. 15). However, the Mg^{2+} affinity of the C347S channels was reduced significantly to an $IC_{50} = 2.8 \text{ mM} \pm 0.6$ ($n = 3$) at +50 mV. We also tried other mutations at this position, including converting C347 into a threonine. Unfortunately, the expression of C347T channels was too small to record reliable currents in excised patches. Mutating C347 to a more radically

different residue, such as to small hydrophobic alanine or glycine residues, in order to further prove that residue 347 contributes to the Mg^{2+} binding site, resulted in non-functional channels. However, the change in affinity with the serine substitution at C347 is consistent with our hypothesis that C347 is part of the Mg^{2+} binding site, deep within the pore domain.

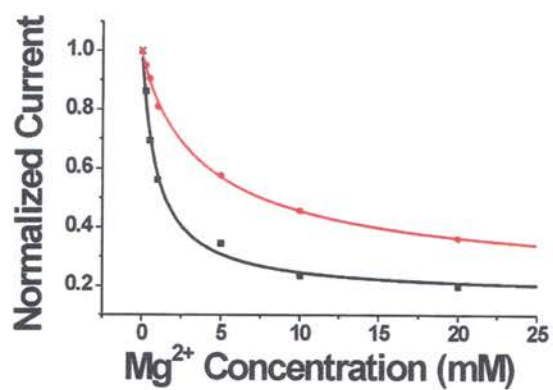


Figure 15. The mutant C347S altered the magnesium affinity in HCN1 channels. Dose response curve for C347 HCN1 channels (■) and C347S HCN1 (●) channels measured as in Figure 5. The data was fitted with the Michael-Menton equation.

e. Magnesium causes inward rectification in a permanently-open HCN channel

In a previous study, the double mutation R318Q/Y331S in HCN2 channels was shown to generate ionic currents with no time dependent component in response to hyperpolarized or depolarized voltage steps [66]. Since the channels did not display any time dependence in their currents in response to hyperpolarizations or depolarizations, the mutant channel was assumed to be in a permanently open state. The authors suggested that mutation R318Q in S4 prevents S4 from moving, while mutation Y331S in the S4-S5 loop decouples S4 from the gate, thereby creating a permanently open channel. However, HCN2 R318Q/Y331S channels still exhibit inward rectifying currents, with larger inward currents than outward currents (Fig 16A). The currents HCN2 R318Q/Y331S channels look very similar to the inward rectifying currents through Kir channels. We tested whether this inward rectification was mainly due to intracellular Mg^{2+} block of the outward currents. Upon patch excision, the outward currents exhibit less rectification and the current/voltage relationship becomes almost linear through all negative and positive potentials (Figs. 16B and 16D), reminiscent of the increase in tail amplitudes seen for WT HCN1 and HCN2 channels after patch excision. The remaining rectification in R318Q/Y331S channels, we attribute to a small time-dependent voltage-activation gated by S4 movement. Application of 1 mM Mg^{2+} was able to restore inward rectification to the currents from R318Q/Y331S channels in excised patches (Figs. 16C and 16D). This ability of

Mg^{2+} to block the outward currents even in a permanently open HCN channel further suggests that Mg^{2+} acts as an extrinsic inward rectifier for outward currents in HCN channels.

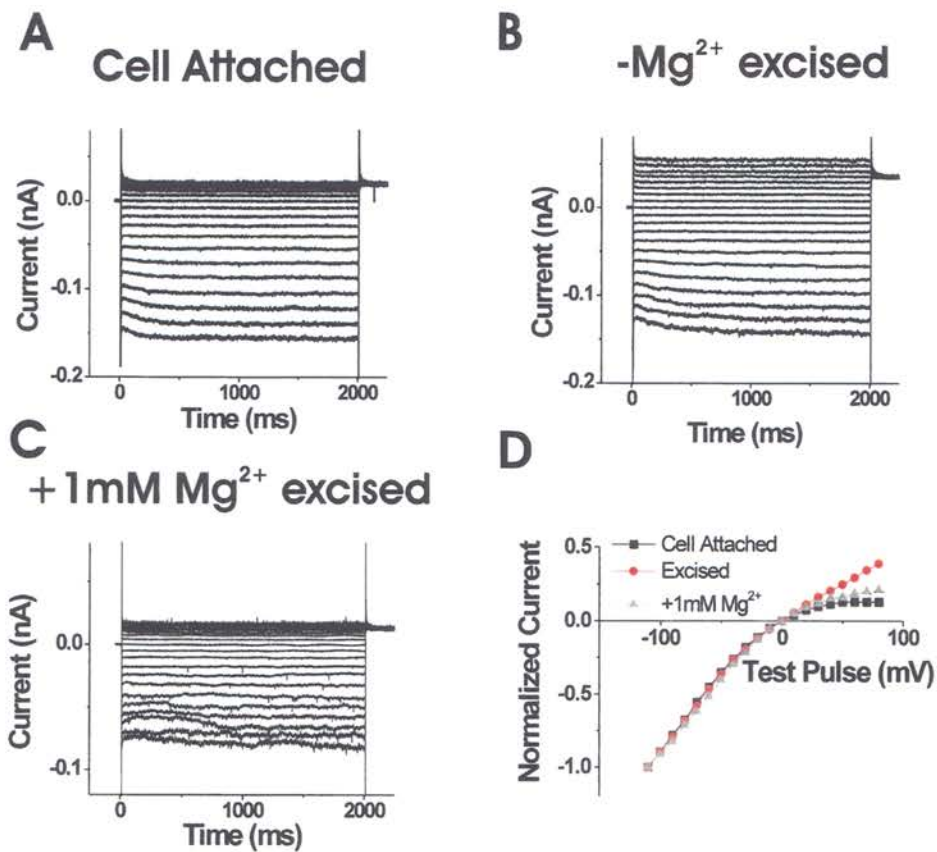


Figure 16. Magnesium causes inward rectification in a permanently-open HCN channel. (A-C). Current from HCN2 R318Q/Y331S channels in response to voltage steps from +80 mV to -110 mV (in -10 mV increments) from a holding potential of 0 mV, followed by a step to $+50$ mV to elicit tail currents. (A) for a cell-attached patch, (B) excised patch with 0 Mg^{2+} applied, and (C) an excised patch after application of 1 mM Mg^{2+} . (D) I/V curves from (A-C) showing inward rectification for ionic currents in cell attached patches (■). The rectification is decreased in an excised patch exposed to 0 Mg^{2+} (●). The rectification is restored, however, upon application of 1 mM Mg^{2+} (▲).

E. Discussion

Using cell-attached and excised patches with HCN1 and HCN2 channels, we have here shown that HCN channels are susceptible to an 'extrinsic' rectification in which intracellular Mg^{2+} blocks the outward currents of HCN channels at positive potentials. Mg^{2+} blocks these outward currents significantly at physiological concentrations with an IC_{50} of 0.53 mM at +50 mV for HCN2 channels. The concentration of free, unbound Mg^{2+} has been estimated to be between 0.5-1.5 mM in the intracellular environment of mammalian cells [104-108], suggesting that the Mg^{2+} block of HCN channels is physiological. The voltage dependence of the Mg^{2+} block suggests a binding site within the transmembrane electric field of HCN channels, presumably in the pore. In the open pore of Kv channels, it is assumed that 80% of the transmembrane electric field primarily lies over the selectivity filter [35, 109]. Therefore, the δ value of .19 obtained for Mg^{2+} of HCN1 channels suggests that the binding site for Mg^{2+} is located internally to the selectivity filter in HCN channels. This location for the Mg^{2+} binding site in HCN channels is consistent with δ values obtained from other channels, for which the binding site for divalent cations such as Mg^{2+} and Ba^{2+} lies in, or close to, the selectivity filter. For instance, in SK2 channels, divalent ions bind with a δ value of 0.39 to a residue in the selectivity filter [110] and, in KcsA, Ba^{2+} binds to the selectivity filter with a δ value of 0.3 [101]. Our mutagenesis of a conserved cysteine located two residues intracellular to the GYG selectivity sequence supports this location for the Mg^{2+} binding site in HCN channels. We showed that mutations of this cysteine altered

the affinity of the binding site, suggesting that this cysteine forms part of the binding site. The 4 cysteines, one from each subunit, form a ring of cysteines at the cytosolic entrance to the selectivity filter [37] and can easily be envisioned to create a binding site for divalent cations (Fig. 17). This cysteine is homologous to a residue in SK channels that has been shown to bind divalent ions in a voltage dependent manner in SK channels [110]. In addition, Vincent Torre's group showed that the same cysteine binds Cd^{2+} in HCN1 channels and that these cysteines can spontaneously crosslink with disulfide bonds, suggesting that these four cysteines are located close together [36]. Sulfur atoms are assumed to bind Mg^{2+} poorly [111]. However, in the crystal structure of the cyanobacterial photosystem I, a Mg^{2+} is shown to be coordinated by a sulfur atom from a methionine [112], and synthetic compounds have been made in which sulfur atoms coordinates Mg^{2+} [113]. The location of four symmetrical located cysteines close together at the entrance to the selectivity filter in HCN channels might form a low-affinity divalent binding site. We assume that the sulfhydryde side chains of the four cysteines in WT HCN channels form a good binding environment for the Mg^{2+} by mimicking waters of hydration. Mutating C347 to a serine or a threonine did change the affinity for Mg^{2+} binding, but did not change binding affinity drastically. However, serine has hydroxyl side chains that could also create a good binding environment for the Mg^{2+} by also mimicking waters of hydration. In the crystal structure of KcsA channels, threonine side chains at the homologous position to C347 contribute to K^+ binding sites in the pore, by mimicking waters of hydration around the K^+ [114].

We were unable to mutate C347 to a more radically different residue, such as to small hydrophobic alanine or glycine residues, to further prove that C347 contributes to the Mg^{2+} binding site. However, the changes in affinity with the serine substitution is consistent with our hypothesis that C347 is part of the Mg^{2+} binding site, deep within the pore domain. The C347 residues are located at the C-terminal end of the pore helices, which have electrical dipoles associated with them that have been suggested to stabilize cations in the pore [115]. These electrical dipoles point their negative poles towards the C347 residues and may also contribute to the binding affinity for Mg^{2+} at this site (Fig. 17). Other residues in the pore cavity might also participate in the coordination of the Mg^{2+} .

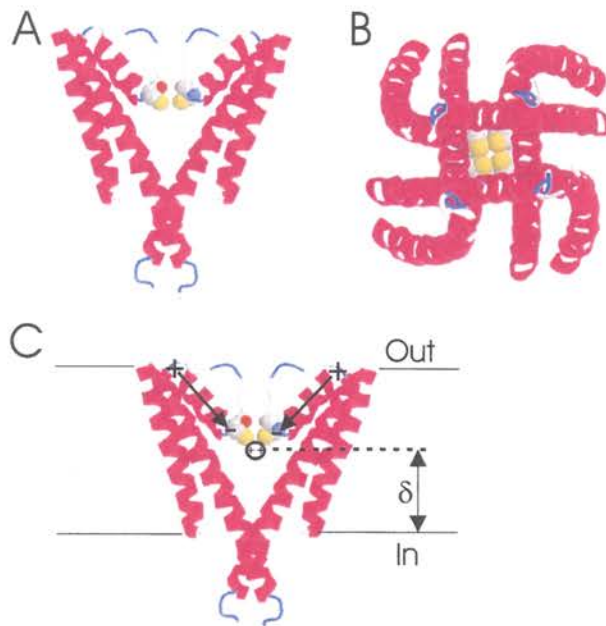


Figure 17. Putative location of the Mg^{2+} binding site in the pore.

Model for the putative binding site for Mg^{2+} in a homology model for the HCN2 channel (modeled after the KcsA crystal structure; [37]), with the four C347 residues highlighted. (A) Side view with only two subunits shown. C347 is shown in space fill. (B) View from the cytosolic side, showing the close proximity of the four C347 side chains in the model. (C) Proposed Mg^{2+} binding site formed by the four C347 at the electrical distance, δ , from the cytosol. The dipoles (arrows) formed by the pore helices may also contribute to the binding affinity for divalent ions, such as Mg^{2+} , to this site.

The voltage-dependent Mg^{2+} block described here for HCN channels creates an 'extrinsic' inward rectification of the instantaneous HCN currents. This is most clearly seen in the Mg^{2+} block of the currents through permanently lock-open HCN channels, which gives rise to currents similar to those through inward rectifying K channels (Kir channels). Kir channels gating properties rely mainly upon the voltage-dependent block by intracellular Mg^{2+} and polyamines (Lopatin 1994). However, HCN channels also possess a major 'intrinsic' gating mechanism in the form of the S4 voltage sensor, which acts to open and close an intracellular activation gate of HCN channels in response to voltage [70]. This voltage-dependent opening and closing of the activation gate is generally assumed to constitute the major voltage-dependent gating mechanism in HCN channels, underlying, for example, the physiological role of HCN channels in pacemaker cells. However, HCN channels exhibit a non-negligible instantaneous current [116], suggested to be contributed by a sub-population of HCN channels that are constitutively open and do not close in response to depolarizations [117]. This 'instantaneous' current, or leak current, through HCN channels, has been proposed to be physiologically important by, for example, increasing the rate of repolarization of plateau action potentials in the heart [117]. The voltage-dependent Mg^{2+} block described here for HCN channels creates an 'extrinsic' inward rectification of these instantaneous currents (Fig. 18) and could prevent too much outward K^+ flow during plateau action potentials that could otherwise prematurely terminate the action potential by this hyperpolarizing K^+ current. In addition, some of the members in the

HCN channel family have very slow kinetics. For example, HCN4 channels open and close with time constants in the seconds [15]. These channels would not have time to all close during a depolarizing action potential. For these slower HCN channels, the Mg^{2+} block might be a faster, secondary voltage-dependent gating mechanism to reduce outward currents through HCN channels at depolarized potentials. Therefore, the Mg^{2+} block in HCN channels might be a mechanism to reduce unwanted outward currents through open HCN channels at prolonged depolarized potentials, such as plateau action potentials.

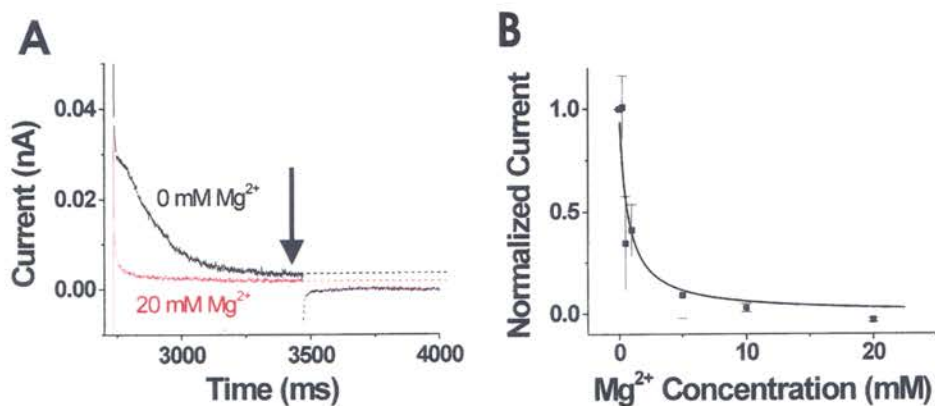


Figure 18. Mg²⁺ blocks a voltage-independent component of the current at positive voltages. (A) Current from an excised patch containing HCN2 channels in response to a +50 mV voltage step, following an -130 mV activation prepulse in the presence or absence of 20 mM Mg²⁺. Holding potential 0 mV. Note that the 20-mM Mg²⁺ solution blocks both the time-dependent HCN2 currents and a time-independent component of the current. The size of time-independent component of the current at +50 mV that was blocked by 20 mM Mg²⁺ was $4.8\% \pm 1.3\%$ ($n = 6$) of the time-dependent HCN2 currents. This is similar to the size of the time-independent currents previously shown in HCN2 channels [117]. (B) Dose response curve for Mg²⁺ block of currents measured at arrow in (A). $IC_{50} = 0.65 \pm 0.26$ ($n = 6$)

IV. Discussion

.The inward rectification in HCN channels is caused by the voltage-dependent movement of S4 and the resulting downstream movements in the channel that act to open and close the channel gate. In addition, the outward currents of HCN channels are blocked by Mg^{2+} in a voltage dependent manner. These two separate methods of inward rectification (S4 working from within the channel, Mg^{2+} coming from the intracellular solution) give rise to the unique functional properties of HCN channels that allow them to perform their physiological duties within the body. These mechanisms of inward rectification, not only reveal more about HCN channel function, but contribute to a greater understanding of ion channel function, particularly the superfamily of voltage-gated ion channels.

A. S4 is the voltage sensor

Previous studies, including this thesis, have shown that S4 is the voltage sensor in spHCN1[70] and the mammalian HCN1 channel[92]. It is reasonable to assume, considering the homology among HCN channels, that S4 is the voltage sensor for the entire HCN channel family. The implications from this conclusion reverberate not just within the HCN channel family, but into the superfamily of voltage-gated ion channels, especially the Kv channels. S4 has been shown to be the voltage sensor for Kv channels as well[54, 55, 72-74], so it is possible that an analysis of S4 movement in HCN channels could reveal

further insight into the mechanics of S4 movement in Kv channels and voltage-gated ion channels in general.

a. S4 movement in HCN1 and Shaker

Depolarization moves S4 outwards in both Shaker and HCN channels, while hyperpolarization moves S4 inwards, towards the intracellular solution, in both channels. Despite this homology of movement, the outcomes are reversed, with the outward movement of S4 opening the Shaker channel and closing the HCN channel. Inward movement of S4 closes the Shaker channel and opens the HCN channel.

A closer inspection of the data concerning S4, finds similarities in the range of S4 movement for both HCN channels and Shaker channels. The use of SCAM identified S4 as the voltage sensor in Shaker channels[55]. Five residues were proposed to lie in the membrane in the closed state, spanning the distance between the intracellular and extracellular solutions. Depolarization is accompanied by the movement of S4 (encompassing up to 9 amino acids) outwards towards the extracellular solution, while allowing more of the S4 domain to remain buried within the membrane[55]. It is proposed that in this open state of S4, electrostatic interactions are formed between S4 and S2-S3 domains[62]. Calculating the predicted gating charge from such a movement results in approximately 3 gating charges per subunit, 12 total for the channel, a number similar to the gating charge per channel calculated for Shaker[53]. This

result was further confirmed by measurements from another paper correlating accessibility changes in the Shaker S4 with the time course and voltage dependence of gating currents[118]. A similar movement of S4 was found for spHCN and HCN1, where the S4 domain translocates across the membrane. The same method (SCAM) was used to define the range of S4 movement, showing that in the open state for HCN, with S4 in the down position, up to 5 residues are buried within the membrane, similar to Shaker. As S4 moves outward, a larger portion of S4 becomes buried within the membrane.

The application of MTSET also reduced the gating current for some of the spHCN1 cysteine mutants, indicating that MTSET was inhibiting the movement of S4 movement, consequently reducing the amount of charge moved through the membrane. This provided further evidence for S4 acting as the voltage sensor.

The gating charge per HCN channel has not been measured, but an estimate from the HCN papers showing S4 movement suggest a total charge moved per S4 domain (~2) similar to Shaker. Interestingly, the same homologous region in Shaker (R368C), spHCN1 (S338C), and HCN1 (S253C/L254C) was found to almost completely translocate across the membrane. The data from Shaker and HCN led to a model where S4, as it moves outward, undergoes a vertical movement, accompanied by a rotation, through the membrane. The lack of state dependence for the N-terminus S4 charges would suggest that these residues do

not undergo a voltage-dependent conformational change or at least do not move through the membrane.

An additional paper about HCN1 was published concerning the movement of HCN1[91]. The results from this paper mostly agree with the work from the first paper included in this thesis. The exception was the lack of state dependence (relative to the state-dependence found in our results: see Chapter 2-discussion) measured for one S4 N-terminus residue (249). This led the authors to propose a model where the transmembrane domains rearrange around S4, therefore altering the shape of the membrane field around it. In this model, S4 stays relatively still. In the open state, S4 lies in a water filled cavity, which collapses when the channel closes.

b. Models for S4 conformational changes

The findings described above, for the most part, suggest a similar movement among all S4 domains in ion channels, but in reality, there is far more data available for Shaker than HCN. Any predictions about the conformational changes for S4 in HCN channels based on Shaker S4 data are speculative. However, this does not preclude the use of Shaker models (as a reference) that were developed to account for structure/function data.

The prevailing model developed from both SCAM studies and fluorescent data[119, 120] proposed that the outward movement of S4 involves a rotation

type of movement, specifically a helical screw motion that occurs in three steps. A rotation movement is also supported from data showing N-terminus S4 charges changing orientation from S2/S3 in the closed state to facing the pore domain in the open state[121]. The S4 is proposed to lie in a groove at the interface between adjacent subunits, facing S5-S6 on one side and S1-S3 on another. This allows S4 charges to move without exposure to the lipid environment. This model can account for S4 data from HCN channels, however, no FRET or electrostatic/interaction studies have been done in HCN to confirm that a helical/rotational type of movement does occur. The inability to record gating currents in mammalian HCN channels also limits the ability to test for potential voltage-dependent intermediate states that S4 may transition into before opening.

Another study replaced S4 charges in Shaker with histidines that were able to conduct protons[122], leading to the model of a gating canal that includes a water pathway connecting the intracellular and extracellular solutions. It is proposed that the gating canal is surrounded on three sides by S2/S3, the pore domain, and lipid[123]. This model suggested a conformational change of structures around a relatively static S4, similar to that for the HCN1 paper proposing a water filled cavity occupied by S4[91].

Many of the functional studies performed on Shaker channels have not been attempted on HCN channels, however, the rotational model of movement for S4

is sufficient to account for what functional data is available for HCN channels[70, 92]. The arrival of crystal structures for 6 trans-membrane domain voltage-gated ion channels was a chance to assess the validity of this model for S4 movement.

c. Crystal Structures

The experimental data from SCAM and gating currents suggest that S4 moves in the same manner between Shaker and HCN channels, however the specifics of such a move are still not known. Structure/function experiments are limited in providing spatial context for defining conformational states of the protein, especially between trans-membrane domains. Several investigators have turned to crystal structures to provide static visual images of proteins. These studies when combined with structure/function studies offer the most promise in explaining the mechanism of gating in voltage gated ion channels.

What did the crystal structures show? The hope in analyzing crystal structures is to see the spatial relationship between the voltage-sensing domain and the pore domain, the very heart of the coupling question. Two crystal structures attempted to achieve this: KvAP, a bacterial channel, and Kv1.2, a mammalian Shaker channel. In both structures, the S1-S4 voltage-sensing domains were found to be at the corners of the pore domains, existing relatively independent (not tightly packed) from the pore domains. The S4 domain lacked the extensive interface with the S5-S6 domain and was attached to the pore domain by the S4-

S5 linker. The voltage sensor was proposed to be a helix-turn-helix structure made up of a portion of the S3 domain and the whole S4 domain[67]. The S4 is shielded by S1-S2 on one side and exposed to lipid on the other[69]. This voltage 'paddle' is proposed to undergo a large movement through the membrane, not within a gating canal surrounded by other channel domains. The coupling mechanism was proposed to be the S4-S5 linker, allowing the movement of S4 to translate into work on the pore[69]. This model does not completely refute the S4 rotational model, in fact, the model for S4 has evolved into a tilted S4 orientation combined with the vertical rotational movement. The more important question, pertaining to this thesis, is how the model is relevant to HCN S4 movement.

The model proposed for S4 movement in KvAP and Kv1.2 show fairly autonomous voltage-sensing domains that are positioned at the corners of the pore domains. The experimental data from SCAM experiments in spHCN and HCN1 do not rule out this possibility. The proposed orientation of S4 in Shaker shielded by S1-S2, also is a possibility for HCN channels, since the negative charges present in Shaker S2 are also present in HCN channels, further suggesting a similar structure for the voltage-sensing domain for HCN and Shaker. The voltage-sensing domain in Shaker has been fused with the KcsA pore to create a functional channel (chimera)[38], bolstering the argument that the voltage-sensing domains are relatively autonomous and do not require an extensive interface with the pore domain. Similar attempts to create chimeras

between HCN1/Shaker and HCN1/Eag (Vemana unpublished observation), were unsuccessful. The difficulty in producing a chimera involving HCN channels would seem to suggest an extensive interface between S4 and the pore domain. In fact, a tryptophan scan of the entire pore domain of Shaker, defined an area between S5-S6 of adjacent subunits as least tolerant to point mutations[124]. S4 was proposed to lie within this groove, a concept contradicted by the crystal structures. Structure/function studies from other inward rectifiers also support the concept of S4 being in close proximity to the pore domain. A random mutagenesis screen for second site suppressors to semilethal mutations in S5, identified two S4 residues that were thought to be in close proximity[125], again arguing against a relatively isolated voltage-sensing domain.

The crystal structure does emphasize the role of the S4-S5 linker in coupling the movement of S4 to the channel gate. The S4-S5 linker is also thought to be important for coupling in HCN channels[66], as it is in Shaker channels. The structural basis for the inverse coupling between HCN and Shaker may lie downstream of S4-S5, in the pore domain. One study found that mutating a S6 glycine into a proline in a bacterial Na⁺ channel shifted the voltage dependence of activation by over -50 mV. The insertion of a proline further encourages the bending of an alpha helix. Interestingly, HCN channels have two glycine residues present in their S6 domain, so perhaps differences in the 'hinge'

properties of S6 between Shaker and HCN channels could account for the inverse coupling.

d. Future Experiments

The ideal experiment for HCN channels is to produce a crystal structure for an HCN channel. A crystal structure, though only a static picture, would provide a foundation for new structure/function experiments. Since no such structures are forthcoming, many of the experiments done in Shaker can be repeated for HCN channels, such as using fluorescence to assess the proximity of S4 to the pore domain. Chimeras have also been attempted for HCN channels, but no functional expression has ever been seen (unpublished observations, personal communication).

B. Mg^{2+} acts as an 'extrinsic' rectifier in HCN channels

The second half of the thesis showed data from experiments using cell-attached and excised patches with HCN1 and HCN2 channels, in which intracellular Mg^{2+} acts as an 'extrinsic' rectifier of HCN current, causing a voltage-dependent block of the outward currents. Mg^{2+} blocks these currents at physiological concentrations, with an IC_{50} of 0.82 mM at +50 mV for HCN1 channels and an IC_{50} of 0.53 mM at +50 mV for HCN2 channels. The concentration of free Mg^{2+} in most mammalian cells ranges from 0.5 to 1.5 mM[104-108].

a. Mg^{2+} inside the cell

Mg^{2+} is the fourth most abundant cation in mammals[107] after Ca^{2+} , K^+ , and Na^+ and plays a significant role in a variety of biological functions. As mentioned earlier, the minimum free concentration of Mg^{2+} in mammalian cells is 0.5mM. Cells possess numerous ways to regulate free Mg^{2+} concentrations, the most important being ATP (adenosine triphosphate) which binds free Mg^{2+} within the cell, forming MgATP. Any process that lowers intracellular ATP levels, such as anoxia, will increase the free Mg^{2+} concentration inside the cell[107]. There is no evidence that Mg^{2+} can bind to cAMP or is affected by changes in intracellular cAMP levels.

b. Mg^{2+} block of ion channels

One of the functions of Mg^{2+} is a regulator of ion channels, including K^+ channels. Mg^{2+} will block the outward currents of Kir channels without any effect on the the inward currents. Kir channels are only made up of two domains making up the equivalent of a pore domain (S5-S6) in Kv channels. Kir does not have a voltage sensor, and depends on the voltage-dependent block by intracellular factors such as Mg^{2+} to cause a rectification of their currents. The extent of Mg^{2+} block of the outward currents can differentiate between types of Kir channels, where complete block of outward currents is seen in strong inward-rectifier channels and incomplete block of outward currents is seen in weak inward rectifiers, such as ROMK1. HCN would most likely be analogous

to a weak inward rectifier channel, considering not all of the outward current is blocked.

In the case of Kir channels, it was found that cytoplasmic polyamines, spermine and spermidine, had a 100 and 10 fold, respectively, greater block than Mg^{2+} [126]. Polyamines were the primary agent of rectification in Kir channels, causing block of outward currents even in the absence of Mg^{2+} . This is not the case for HCN channels, where Mg^{2+} had a 4-fold and 2-fold greater block than spermine and spermidine, respectively, for HCN outward currents. Interestingly, the length of the polyamine is directly related to the extent of block. This is also seen for HCN channels, where spermidine blocks more outward current than spermine, implying some similarities in the pore domain between the two channels, or at the very least, a similar blocking mechanism. This is significant because it is proposed that polyamines and Mg^{2+} share the same binding sites in Kir channels[126].

c. Mechanism of HCN block by Mg^{2+}

Mg^{2+} blocks HCN outward currents in a voltage dependent manner, just as in Kir channels. The δ value of .19 for HCN, suggests a binding site within the transmembrane electric field of HCN channels. In Kv channels, it is thought that 80% of the transmembrane electric field lies over the selectivity filter[35, 109]. This would place the Mg^{2+} binding site internal to the HCN selectivity filter. This is similar to δ values for other channels, like the δ value of .39 for divalent

ions in SK channels and the δ value of .3 for Ba^{2+} in KcsA. Mutation of a cysteine residue located two residues intracellular to the GYG selectivity in HCN channels reduced the affinity for Mg^{2+} . This cysteine forms a ring below the selectivity filter, at the cytosolic entrance, creating a potential binding site for divalent cations like Mg^{2+} . The location of the proposed Mg^{2+} binding site, is supported by data from HCN1 channels showing that these cysteines can coordinate the binding of Cd^{2+} and spontaneously crosslink with disulfide bonds. This would support the idea that these four cysteines in HCN1 are located very close together. The coordination of Mg^{2+} by cysteines is not common but has precedent. (please refer back to chapter 3 section D). The presence of a low affinity binding site in the selectivity filter of HCN channels would explain the incomplete block of outward currents and suggest that the HCN channel pore might be similar to weak inward rectifiers, such as ROMK1.

d. Mg^{2+} and HCN, the physiological significance

HCN channels are primarily gated by their 'intrinsic' gating mechanism in the form of S4. The voltage-dependent movement of HCN S4 activates and deactivates currents through the pore. This current underlies the role of HCN channels as 'pacemakers' in the body. HCN channels, however, also display a voltage-independent current, that is thought to be mediated by a distinct population of HCN channels that are constitutively open, even during depolarizations[117]. This voltage-independent time-independent current would potentially accelerate both depolarization and repolarization. By blocking this

voltage-independent current Mg^{2+} can delay the premature onset of repolarization during a plateau action potential. HCN4 channels, for instance, open and close on a time scale of seconds and would not all close during a depolarization step. Mg^{2+} block of the outward current through open HCN4 channels would act as a supplemental voltage-dependent gating mechanism.

e. Future Experiments

HCN channels are very sensitive to mutations within their selectivity filter, and have prevented experiments looking at the effect of substituting cysteine with other amino acids. The results from such experiments could provide further evidence for the cysteine as the primary location for Mg^{2+} or produce changes in the δ value, suggesting a secondary binding site for Mg^{2+} . It would also be interesting to assess the effect of a negative charge in the selectivity filter. The introduction of a negative charge into the pore domain of a ROMK1 converted this channel from a weak inward rectifier into a strong inward rectifier[102]. Another consideration, is the effect on the voltage-dependent block of Mg^{2+} by changing the concentration of extracellular K^+ . It has been shown in Kir channels, that raising the extracellular K^+ levels decreases Mg^{2+} affinity. A similar effect on HCN channels, would further support the notion of Mg^{2+} blocking the pore.

V. Summary and Conclusions

The experiments contained within this thesis show evidence that HCN channels are gated by the voltage-dependent movement of S4, which acts as the voltage sensor, and by the voltage-dependent block by intracellular Mg^{2+} ions. The data supporting these conclusions comes primarily from two-electrode voltage clamp/SCAM and patch clamp experiments.

S4 was found to move outwards in response to depolarization and inwards in response to hyperpolarization, based on the state-dependent accessibility of cysteine mutants to cysteine reactive compounds such as MTSET. The region around residue, S253C, was found to almost completely translocate across the membrane. This movement of S4 is coupled to the opening and closing of the intracellular channel gate by an unknown mechanism.

The S4 gating in HCN1 is complemented by the action of intracellular Mg^{2+} , which acts to block the outward currents of HCN channels in a voltage-dependent manner. This behavior suggests a binding site within the transmembrane electric field of the HCN channel, presumably localized to a cysteine just below the selectivity filter, based on the reduced Mg^{2+} affinity of HCN channels when this cysteine is removed. In addition, Mg^{2+} blocks both the time-dependent and time-independent outward currents in HCN channels. This block may play a physiological role in preventing the outward current of HCN channels from prematurely terminating the plateau of a cardiac action potential.

This thesis makes a contribution to the field of voltage-dependent ion channels, specifically HCN channels. Ultimately, these findings will aid in the development of a comprehensive explanation for the gating mechanisms in HCN channels.

VI. References

1. Hodgkin, A.L. and A.F. Huxley, *A quantitative description of membrane current and its application to conduction and excitation in nerve*. J Physiol, 1952. **117**(4): p. 500-44.
2. Cole, K.S.a.H.J.C., *Electrical Impedance of the squid giant axon during activity*. Journal of General Physiology, 1939. **22**: p. 649-670.
3. Brown, H., D. DiFrancesco, and S. Noble, *Cardiac pacemaker oscillation and its modulation by autonomic transmitters*. J Exp Biol, 1979. **81**: p. 175-204.
4. Yanagihara, K. and H. Irisawa, *Inward current activated during hyperpolarization in the rabbit sinoatrial node cell*. Pflugers Arch, 1980. **385**(1): p. 11-9.
5. DiFrancesco, D., *Pacemaker mechanisms in cardiac tissue*. Annu Rev Physiol, 1993. **55**: p. 455-72.
6. Pape, H.C., *Queer current and pacemaker: the hyperpolarization-activated cation current in neurons*. Annu Rev Physiol, 1996. **58**: p. 299-327.
7. Maylie, J., et al., *A study of pace-maker potential in rabbit sino-atrial node: measurement of potassium activity under voltage-clamp conditions* J Physiol., 1981. **311**(1 Suppl): p. 161-78.
8. DiFrancesco, D., *A study of the ionic nature of the pace-maker current in calf Purkinje fibres*. J Physiol, 1981. **314**: p. 377-93.
9. DiFrancesco, D., et al., *Properties of the hyperpolarizing-activated current (I_h) in cells isolated from the rabbit sino-atrial node*. J Physiol, 1986. **377**: p. 61-88.
10. DiFrancesco, D., *Characterization of the pace-maker current kinetics in calf Purkinje fibres*. J Physiol, 1984. **348**: p. 341-67.
11. Morad, M. and J. Maylie, *Calcium and cardiac electrophysiology. Some experimental considerations*. Chest, 1980. **78**(1 Suppl): p. 166-73.
12. Brown, H.F., et al., *The ionic currents underlying pacemaker activity in rabbit sino-atrial node: experimental results and computer simulations*. Proc R Soc Lond B Biol Sci, 1984. **222**(1228): p. 329-47.
13. Halliwell, J.V. and P.R. Adams, *Voltage-clamp analysis of muscarinic excitation in hippocampal neurons*. Brain Res, 1982. **250**(1): p. 71-92.
14. Attwell, D. and M. Wilson, *Behaviour of the rod network in the tiger salamander retina mediated by membrane properties of individual rods*. J Physiol, 1980. **309**: p. 287-315.
15. Santoro, B. and G.R. Tibbs, *The HCN gene family: molecular basis of the hyperpolarization-activated pacemaker channels*. Ann N Y Acad Sci, 1999. **868**: p. 741-64.
16. Ludwig, A., et al., *A family of hyperpolarization-activated mammalian cation channels*. Nature, 1998. **393**(6685): p. 587-91.

17. Vaccari, T., et al., *The human gene coding for HCN2, a pacemaker channel of the heart*. Biochim Biophys Acta, 1999. **1446**(3): p. 419-25.
18. Gaus, R., R. Seifert, and U.B. Kaupp, *Molecular identification of a hyperpolarization-activated channel in sea urchin sperm*. Nature, 1998. **393**(6685): p. 583-7.
19. Galindo, B.E., A.T. Neill, and V.D. Vacquier, *A new hyperpolarization-activated, cyclic nucleotide-gated channel from sea urchin sperm flagella*. Biochem Biophys Res Commun, 2005. **334**(1): p. 96-101.
20. Mistrik, P., et al., *The murine HCN3 gene encodes a hyperpolarization-activated cation channel with slow kinetics and unique response to cyclic nucleotides*. J Biol Chem, 2005. **280**(29): p. 27056-61.
21. Stieber, J., et al., *Functional expression of the human HCN3 channel*. J Biol Chem, 2005. **280**(41): p. 34635-43.
22. Ishii, T.M., M. Takano, and H. Ohmori, *Determinants of activation kinetics in mammalian hyperpolarization-activated cation channels*. J Physiol, 2001. **537**(Pt 1): p. 93-100.
23. Ishii, T.M., et al., *Peripheral N- and C-terminal domains determine deactivation kinetics of HCN channels*. Biochem Biophys Res Commun, 2007. **359**(3): p. 592-8.
24. Stieber, J., et al., *Molecular basis for the different activation kinetics of the pacemaker channels HCN2 and HCN4*. J Biol Chem, 2003. **278**(36): p. 33672-80.
25. Robinson, R.B. and S.A. Siegelbaum, *Hyperpolarization-Activated Cation Currents: From Molecules to Physiological Function*. Annu Rev Physiol, 2003. **65**: p. 453-80.
26. DiFrancesco, D. and P. Tortora, *Direct activation of cardiac pacemaker channels by intracellular cyclic AMP*. Nature, 1991. **351**(6322): p. 145-7.
27. Santoro, B., et al., *Molecular and functional heterogeneity of hyperpolarization-activated pacemaker channels in the mouse CNS*. J Neurosci, 2000. **20**(14): p. 5264-75.
28. Ulens, C. and J. Tytgat, *Functional heteromerization of HCN1 and HCN2 pacemaker channels*. J Biol Chem, 2001. **276**(9): p. 6069-72.
29. Beaumont, V. and R.S. Zucker, *Enhancement of synaptic transmission by cyclic AMP modulation of presynaptic Ih channels*. Nat Neurosci, 2000. **3**(2): p. 133-41.
30. Ludwig, A., et al., *Absence epilepsy and sinus dysrhythmia in mice lacking the pacemaker channel HCN2*. Embo J, 2003. **22**(2): p. 216-24.
31. Yu, X., et al., *Calcium influx through hyperpolarization-activated cation channels (I(h) channels) contributes to activity-evoked neuronal secretion*. Proc Natl Acad Sci U S A., 2004. **101**(4): p. 1051-6. Epub 2004 Jan 14.
32. Shin, K., B. Rothberg, and G. Yellen, *Blocker State Dependence and Trapping in Hyperpolarization-activated Cation Channels. Evidence for an intracellular activation gate*. J Gen Physiol, 2001. **117**(2): p. 91-102.
33. Biel, M., et al., *Hyperpolarization-activated cation channels: a multi-gene family*. Rev Physiol Biochem Pharmacol, 1999. **136**: p. 165-81.

34. Wahl-Schott, C., et al., *An arginine residue in the pore region is a key determinant of chloride dependence in cardiac pacemaker channels* J Biol Chem., 2005. **280**(14): p. 13694-700. Epub 2005 Jan 10.
35. Doyle, D.A., et al., *The structure of the potassium channel: molecular basis of K⁺ conduction and selectivity*. Science, 1998. **280**(5360): p. 69-77.
36. Roncaglia, P., P. Mistrik, and V. Torre, *Pore topology of the hyperpolarization-activated cyclic nucleotide-gated channel from sea urchin sperm*. Biophys J., 2002. **83**(4): p. 1953-64.
37. Giorgetti, A., et al., *A homology model of the pore region of HCN channels*. Biophys J, 2005. **89**(2): p. 932-44.
38. Lu, Z., A.M. Klem, and Y. Ramu, *Ion conduction pore is conserved among potassium channels*. Nature, 2001. **413**(6858): p. 809-13.
39. Jiang, Y., et al., *The open pore conformation of potassium channels*. Nature, 2002. **417**(6888): p. 523-6.
40. Rothberg, B.S., et al., *Voltage-controlled gating at the intracellular entrance to a hyperpolarization-activated cation channel*. J Gen Physiol, 2002. **119**(1): p. 83-91.
41. Osterrieder, W., et al., *Injection of subunits of cyclic AMP-dependent protein kinase into cardiac myocytes modulates Ca²⁺ current*. Nature, 1982. **298**(5874): p. 576-8.
42. Wainger, B.J., et al., *Molecular mechanism of cAMP modulation of HCN pacemaker channels*. Nature, 2001. **411**(6839): p. 805-10.
43. Wang, J., S. Chen, and S.A. Siegelbaum, *Regulation of hyperpolarization-activated HCN channel gating and cAMP modulation due to interactions of COOH terminus and core transmembrane regions*. J Gen Physiol, 2001. **118**(3): p. 237-50.
44. Zagotta, W.N., et al., *Structural basis for modulation and agonist specificity of HCN pacemaker channels*. Nature, 2003. **425**(6954): p. 200-5.
45. Hille, B., *Ion Channels of Excitable Membranes*. Third ed. 2001: Sinauer.
46. Tempel, B.L., Y.N. Jan, and L.Y. Jan, *Cloning of a probable potassium channel gene from mouse brain*. Nature, 1988. **332**(6167): p. 837-9.
47. MacKinnon, R., *Determination of the subunit stoichiometry of a voltage-activated potassium channel*. Nature, 1991. **350**(6315): p. 232-5.
48. Armstrong, C.M. and F. Bezanilla, *Currents related to movement of the gating particles of the sodium channels*. Nature., 1973. **242**(5398): p. 459-61.
49. Stuhmer, W., et al., *Structural parts involved in activation and inactivation of the sodium channel*. Nature., 1989. **339**(6226): p. 597-603.
50. Perozo, E., et al., *S4 mutations alter gating currents of Shaker K channels*. Biophys J, 1994. **66**(2 Pt 1): p. 345-54.
51. Papazian, D.M., et al., *Alteration of voltage-dependence of Shaker potassium channel by mutations in the S4 sequence*. Nature, 1991. **349**(6307): p. 305-10.
52. Bezanilla, F., et al., *Molecular basis of gating charge immobilization in Shaker potassium channels*. Science, 1991. **254**(5032): p. 679-83.
53. Schoppa, N.E., et al., *The size of gating charge in wild-type and mutant Shaker potassium channels*. Science, 1992. **255**(5052): p. 1712-5.

54. Aggarwal, S.K. and R. MacKinnon, *Contribution of the S4 segment to gating charge in the Shaker K⁺ channel*. Neuron, 1996. **16**(6): p. 1169-77.
55. Larsson, H.P., et al., *Transmembrane movement of the shaker K⁺ channel S4*. Neuron, 1996. **16**(2): p. 387-97.
56. Smith, P.L., T. Baukrowitz, and G. Yellen, *The inward rectification mechanism of the HERG cardiac potassium channel*. Nature, 1996. **379**(6568): p. 833-6.
57. Miller, A.G. and R.W. Aldrich, *Conversion of a delayed rectifier K⁺ channel to a voltage-gated inward rectifier K⁺ channel by three amino acid substitutions*. Neuron, 1996. **16**(4): p. 853-8.
58. Zei, P.C. and R.W. Aldrich, *Voltage-dependent gating of single wild-type and S4 mutant KAT1 inward rectifier potassium channels*. J Gen Physiol, 1998. **112**(6): p. 679-713.
59. Chen, J., et al., *Functional roles of charged residues in the putative voltage sensor of the HCN2 pacemaker channel*. J Biol Chem, 2000. **275**(46): p. 36465-71.
60. Vaca, L., et al., *Mutations in the S4 domain of a pacemaker channel alter its voltage dependence*. FEBS Lett, 2000. **479**(1-2): p. 35-40.
61. Papazian, D.M., et al., *Electrostatic interactions of S4 voltage sensor in Shaker K⁺ channel*. Neuron., 1995. **14**(6): p. 1293-301.
62. Tiwari-Woodruff, S.K., et al., *Electrostatic interactions between transmembrane segments mediate folding of Shaker K⁺ channel subunits*. Biophys J, 1997. **72**(4): p. 1489-500.
63. McCormack, K., et al., *A role for hydrophobic residues in the voltage-dependent gating of Shaker K⁺ channels*. Proc Natl Acad Sci U S A., 1991. **88**(7): p. 2931-5.
64. Shieh, C.C., K.G. Klemic, and G.E. Kirsch, *Role of transmembrane segment S5 on gating of voltage-dependent K⁺ channels*. J Gen Physiol., 1997. **109**(6): p. 767-78.
65. Sanguinetti, M.C. and Q.P. Xu, *Mutations of the S4-S5 linker alter activation properties of HERG potassium channels expressed in Xenopus oocytes*. J Physiol, 1999. **514**(Pt 3): p. 667-75.
66. Chen, J., et al., *The S4-S5 linker couples voltage sensing and activation of pacemaker channels*. Proc Natl Acad Sci U S A, 2001. **98**(20): p. 11277-82.
67. Jiang, Y., et al., *X-ray structure of a voltage-dependent K⁺ channel*. Nature, 2003. **423**(6935): p. 33-41.
68. Jiang, Y., et al., *The principle of gating charge movement in a voltage-dependent K⁺ channel*. Nature., 2003. **423**(6935): p. 42-8.
69. Long, S.B., E.B. Campbell, and R. Mackinnon, *Crystal Structure of a Mammalian Voltage-Dependent Shaker Family K⁺ Channel*. Science, 2005. **7**: p. 7.
70. Mannikko, R., F. Elinder, and H.P. Larsson, *Voltage-sensing mechanism is conserved among ion channels gated by opposite voltages*. Nature, 2002. **419**(6909): p. 837-41.
71. Sesti, F., et al., *Hyperpolarization moves S4 sensors inward to open MVP, a methanococcal voltage-gated potassium channel*. Nat Neurosci, 2003. **6**(4): p. 353-61.

72. Baker, O.S., et al., *Three transmembrane conformations and sequence-dependent displacement of the S4 domain in shaker K⁺ channel gating*. *Neuron*, 1998. **20**(6): p. 1283-94.
73. Seoh, S.A., et al., *Voltage-sensing residues in the S2 and S4 segments of the Shaker K⁺ channel*. *Neuron*, 1996. **16**(6): p. 1159-67.
74. Yusaf, S.P., D. Wray, and A. Sivaprasadarao, *Measurement of the movement of the S4 segment during the activation of a voltage-gated potassium channel*. *Pflugers Arch*, 1996. **433**(1-2): p. 91-7.
75. Xue, T., E. Marban, and R.A. Li, *Dominant-negative suppression of HCN1- and HCN2-encoded pacemaker currents by an engineered HCN1 construct: insights into structure-function relationships and multimerization*. *Circ Res*, 2002. **90**(12): p. 1267-73.
76. Maller, J.L., F.R. Butcher, and E.G. Krebs, *Early effect of progesterone on levels of cyclic adenosine 3':5'- monophosphate in Xenopus oocytes*. *J Biol Chem*, 1979. **254**(3): p. 579-82.
77. Bell, D.C.a.S.A.S. 2002: New York.
78. Karlin, A. and M.H. Akabas, *Substituted-cysteine accessibility method*. *Methods Enzymol*, 1998. **293**: p. 123-45.
79. Sigworth, Y.a. 2002: Palo Alto.
80. Holmgren, M., et al., *On the use of thiol-modifying agents to determine channel topology*. *Neuropharmacology*, 1996. **35**(7): p. 797-804.
81. Stauffer, D.A. and A. Karlin, *Electrostatic potential of the acetylcholine binding sites in the nicotinic receptor probed by reactions of binding-site cysteines with charged methanethiosulfonates*. *Biochemistry*, 1994. **33**(22): p. 6840-9.
82. Schoppa, N.E. and F.J. Sigworth, *Activation of Shaker potassium channels. III. An activation gating model for wild-type and V2 mutant channels*. *J Gen Physiol*, 1998. **111**(2): p. 313-42.
83. Mannuzzu, L.M. and E.Y. Isacoff, *Independence and cooperativity in rearrangements of a potassium channel voltage sensor revealed by single subunit fluorescence*. *J Gen Physiol*, 2000. **115**(3): p. 257-68.
84. Loboda, A. and C.M. Armstrong, *Resolving the gating charge movement associated with late transitions in K channel activation*. *Biophys J*, 2001. **81**(2): p. 905-16.
85. Larsson, H.P., *The search is on for the voltage sensor-to-gate coupling*. *J Gen Physiol*, 2002. **120**(4): p. 475-81.
86. Santoro, B., et al., *Identification of a gene encoding a hyperpolarization-activated pacemaker channel of brain*. *Cell*, 1998. **93**(5): p. 717-29.
87. Nolan, M.F., et al., *The hyperpolarization-activated HCN1 channel is important for motor learning and neuronal integration by cerebellar Purkinje cells*. *Cell*, 2003. **115**(5): p. 551-64.
88. Schulze-Bahr, E., et al., *Pacemaker channel dysfunction in a patient with sinus node disease*. *J Clin Invest*, 2003. **111**(10): p. 1537-45.
89. Ueda, K., et al., *Functional characterization of a trafficking-defective HCN4 mutation, D553N, associated with cardiac arrhythmia*. *J Biol Chem*, 2004. **279**(26): p. 27194-8.

90. Rothberg, B.S., K.S. Shin, and G. Yellen, *Movements near the gate of a hyperpolarization-activated cation channel*. J Gen Physiol, 2003. **122**(5): p. 501-10.
91. Bell, D.C., et al., *Changes in local S4 environment provide a voltage-sensing mechanism for mammalian hyperpolarization-activated HCN channels*. J Gen Physiol, 2004. **123**(1): p. 5-19. Epub 2003 Dec 15.
92. Vemana, S., S. Pandey, and H.P. Larsson, *S4 movement in a mammalian HCN channel*. J Gen Physiol, 2004. **123**(1): p. 21-32. Epub 2003 Dec 15.
93. Baruscotti, M., A. Bucchi, and D. DiFrancesco, *Physiology and pharmacology of the cardiac pacemaker ("funny") current*. Pharmacol Ther, 2005. **107**(1): p. 59-79.
94. Kramer, R.H., *Patch cramming: monitoring intracellular messengers in intact cells with membrane patches containing detector ion channels*. Neuron., 1990. **4**(3): p. 335-41.
95. Pian, P., et al., *Regulation of gating and rundown of HCN hyperpolarization-activated channels by exogenous and endogenous PIP2*. J Gen Physiol, 2006. **128**(5): p. 593-604.
96. Lu, Z., *Mechanism of rectification in inward-rectifier K⁺ channels*. Annu Rev Physiol, 2004. **66**: p. 103-29.
97. Nichols, C.G. and A.N. Lopatin, *Inward rectifier potassium channels*. Annu Rev Physiol, 1997. **59**: p. 171-91.
98. Miyamoto, S., et al., *Estimation of polyamine distribution and polyamine stimulation of protein synthesis in Escherichia coli*. Arch Biochem Biophys., 1993. **300**(1): p. 63-8.
99. Yan, D.H., et al., *Different intracellular polyamine concentrations underlie the difference in the inward rectifier K⁽⁺⁾ currents in atria and ventricles of the guinea-pig heart*. J Physiol., 2005. **563**(Pt 3): p. 713-24. Epub 2005 Jan 24.
100. Woodhull, A.M., *Ionic blockage of sodium channels in nerve*. J Gen Physiol, 1973. **61**(6): p. 687-708.
101. Jiang, Y. and R. MacKinnon, *The barium site in a potassium channel by x-ray crystallography*. J Gen Physiol, 2000. **115**(3): p. 269-72.
102. Lu, Z., et al., *Electrostatic tuning of Mg²⁺ affinity in an inward-rectifier K⁺ channel* Nature., 1994. **371**(6494): p. 243-6.
103. Wible, B.A., et al., *Gating of inwardly rectifying K⁺ channels localized to a single negatively charged residue*. Nature, 1994. **371**(6494): p. 246-9.
104. Kim, S.J., et al., *Ketamine-induced cardiac depression is associated with increase in [Mg²⁺]_i and activation of p38 MAP kinase and ERK 1/2 in guinea pig*. Biochem Biophys Res Commun, 2006. **349**(2): p. 716-22.
105. Almulla, H.A., et al., *Loading rat heart myocytes with Mg²⁺ using low-[Na⁺] solutions*. J Physiol, 2006. **575**(Pt 2): p. 443-54.
106. Csernoch, L., et al., *Measurements of intracellular Mg²⁺ concentration in mouse skeletal muscle fibers with the fluorescent indicator mag-indo-1*. Biophys J, 1998. **75**(2): p. 957-67.
107. Romani, A., *Regulation of magnesium homeostasis and transport in mammalian cells*. Arch Biochem Biophys, 2007. **458**(1): p. 90-102.

108. Handy, R.D., et al., *Na-dependent regulation of intracellular free magnesium concentration in isolated rat ventricular myocytes*. J Mol Cell Cardiol, 1996. **28**(8): p. 1641-51.
109. Yellen, G., et al., *Mutations affecting internal TEA blockade identify the probable pore-forming region of a K⁺ channel*. Science, 1991. **251**(4996): p. 939-42.
110. Soh, H. and C.S. Park, *Localization of divalent cation-binding site in the pore of a small conductance Ca(2+)-activated K(+) channel and its role in determining current-voltage relationship*. Biophys J., 2002. **83**(5): p. 2528-38.
111. Dudev, T., et al., *First-second shell interactions in metal binding sites in proteins: a PDB survey and DFT/CDM calculations*. J Am Chem Soc, 2003. **125**(10): p. 3168-80.
112. Jordan, P., et al., *Three-dimensional structure of cyanobacterial photosystem I at 2.5 Å resolution*. Nature, 2001. **411**(6840): p. 909-17.
113. Sousa Pedrares, A., W. Teng, and K. Ruhlandt-Senge, *Syntheses and structures of magnesium pyridine thiolates--model compounds for magnesium binding in photosystem I*. Chemistry, 2003. **9**(9): p. 2019-24.
114. Zhou, Y., et al., *Chemistry of ion coordination and hydration revealed by a K⁺ channel-Fab complex at 2.0 Å resolution*. Nature, 2001. **414**(6859): p. 43-8.
115. Roux, B. and R. MacKinnon, *The cavity and pore helices in the KcsA K⁺ channel: electrostatic stabilization of monovalent cations*. Science, 1999. **285**(5424): p. 100-2.
116. Proenza, C., et al., *Pacemaker channels produce an instantaneous current*. J Biol Chem, 2002. **277**(7): p. 5101-9.
117. Proenza, C. and G. Yellen, *Distinct populations of HCN pacemaker channels produce voltage-dependent and voltage-independent currents*. J Gen Physiol, 2006. **127**(2): p. 183-90.
118. Mannuzzu, L.M., M.M. Moronne, and E.Y. Isacoff, *Direct physical measure of conformational rearrangement underlying potassium channel gating*. Science, 1996. **271**(5246): p. 213-6.
119. Cha, A., et al., *Atomic scale movement of the voltage-sensing region in a potassium channel measured via spectroscopy*. Nature, 1999. **402**(6763): p. 809-13.
120. Glauner, K.S., et al., *Spectroscopic mapping of voltage sensor movement in the Shaker potassium channel*. Nature, 1999. **402**(6763): p. 813-7.
121. Elinder, F., R. Mannikko, and H.P. Larsson, *S4 charges move close to residues in the pore domain during activation in a K channel*. J Gen Physiol, 2001. **118**(1): p. 1-10.
122. Starace, D.M., E. Stefani, and F. Bezanilla, *Voltage-dependent proton transport by the voltage sensor of the Shaker K⁺ channel*. Neuron, 1997. **19**(6): p. 1319-27.
123. Gandhi, C.S. and E.Y. Isacoff, *Molecular models of voltage sensing*. J Gen Physiol, 2002. **120**(4): p. 455-63.
124. Li-Smerin, Y., D.H. Hackos, and K.J. Swartz, *A localized interaction surface for voltage-sensing domains on the pore domain of a K⁺ channel*. Neuron, 2000. **25**(2): p. 411-23.

125. Lai, H.C., et al., *The S4 voltage sensor packs against the pore domain in the KAT1 voltage-gated potassium channel*. *Neuron*, 2005. **47**(3): p. 395-406.
126. Lopatin, A.N., E.N. Makhina, and C.G. Nichols, *Potassium channel block by cytoplasmic polyamines as the mechanism of intrinsic rectification*. *Nature*, 1994. **372**(6504): p. 366-9.